NASA Technical Paper 1689

Control-System Techniques for Improved Departure/Spin Resistance for Fighter Aircraft

Luat T. Nguyen, William P. Gilbert,
and Marilyn E. Ogburn

AUGUST 1980

NASA

NASA Technical Paper 1689

Control-System Techniques for Improved Departure/Spin Resistance for Fighter Aircraft

Luat T. Nguyen, William P. Gilbert,
and Marilyn E. Ogburn
Langley Research Center
Hampton, Virginia

National Aeronautics
and Space Administration

**Scientific and Technical
Information Branch**

1980

SUMMARY

This paper summarizes some fundamental information on control-system effects on controllability of highly maneuverable aircraft at high angles of attack and techniques for enhancing fighter aircraft departure/spin resistance using control-system design. The discussion includes (1) a brief review of pertinent high-angle-of-attack phenomena including aerodynamics, inertia coupling, and kinematic coupling, (2) effects of conventional stability augmentation systems at high angle of attack, (3) high-angle-of-attack control-system concepts designed to enhance departure/spin resistance, and (4) the outlook for applications of these concepts to future fighters, particularly those designs which incorporate relaxed static stability.

INTRODUCTION

Designers of modern fighter aircraft are faced with the requirement of providing extreme maneuverability and a high level of departure/spin resistance. Two general design approaches are followed to attain this goal. These are (1) aerodynamic design, which involves detailed configuring of the basic airframe geometry to provide inherently good high-angle-of-attack characteristics, and (2) control-system design. In recent years, increasing emphasis has been placed on the second approach because of rapid advances in avionic technology which have made the implementation of complex control laws more practical. As a result of this design philosophy, modern fighters such as the F-15, F-16, and F-18 all incorporate control-system features that enhance maneuverability at high angles of attack and greatly reduce susceptibility to departures and spins.

Because of its unique testing techniques and experience in stall/spin technology, the NASA Langley Research Center has been active in developing the use of control-system design to enhance the departure/spin resistance of fighter aircraft. This paper is a summary of the experience gained at Langley in this area as a result of numerous piloted simulation studies, subscale dynamic model tests, and full-scale flight tests of modern fighter aircraft. Some fundamental high-angle-of-attack aerodynamic, inertia-coupling, and kinematic-coupling phenomena are reviewed to establish some of the basic factors involved. Next, the effect on spin resistance of conventional stability augmentation systems not designed for high-angle-of-attack flight conditions is addressed. Simple roll and yaw dampers, for example, fall into this category and, although they are generally

low-gain, limited-authority devices, their effects on departure/spin resistance can be significant. Next, specific high-angle-of-attack control concepts, many of which are currently being used in the latest fighters, are discussed. These concepts include control crossfeeding, stability-axis yaw damping, static stability augmentation, angle-of-attack limiting, and automatic spin prevention. The rationale for each system is discussed and the advantages and potential limitations are reviewed. Finally, application of the technique to future configurations incorporating advanced concepts such as relaxed static longitudinal stability is addressed. The analysis presented in this paper is conducted using a set of aerodynamic stability and control and inertial characteristics that are representative of many current fighter airplane designs. In this report, this set of aerodynamic and inertial characteristics is referred to as the fighter configuration, the basic configuration, or a similar description.

SYMBOLS

All aerodynamic data and flight motions are referenced to the body system of axes shown in figure 1. The units for physical quantities used herein are presented in the International System of Units (SI) and U.S. Customary Units. The measurements and calculations were made in U.S. Customary Units.

a_n normal acceleration, positive along negative Z body axis, g units ($1g = 9.8\ m/sec^2$)

b wing span, m (ft)

C_L lift coefficient, $\dfrac{\text{Aerodynamic lift force}}{\bar{q}S}$

C_l rolling-moment coefficient about X body axis, $\dfrac{\text{Aerodynamic rolling moment}}{\bar{q}Sb}$

C_m pitching-moment coefficient about Y body axis, $\dfrac{\text{Aerodynamic pitching moment}}{\bar{q}S\bar{c}}$

C_n yawing-moment coefficient about Z body axis, $\dfrac{\text{Aerodynamic yawing moment}}{\bar{q}Sb}$

C_Y Y-axis force coefficient along positive Y body axis, $\frac{\text{Aerodynamic Y-axis force}}{\bar{q}S}$

$\bar{c}$ wing mean aerodynamic chord, m (ft)

g acceleration due to gravity, m/sec^2 (ft/sec^2)

h altitude, m (ft)

I_X, I_Y, I_Z moments of inertia about X, Y, and Z body axes, $kg\text{-}m^2$ ($slug\text{-}ft^2$)

K gearing ratio between yaw and roll controls

K_p static gain, deg/(deg/sec)

K_β static gain, deg/deg

M Mach number

M_{ic} pitching moment due to inertia coupling, $\left(I_Z - I_X\right)pr$, N-m (ft-lb)

N_{ic} yawing moment due to inertia coupling, $\left(I_X - I_Y\right)pq$, N-m (ft-lb)

m airplane mass, kg (slugs)

$p^*_{s,1}, p^*_{s,2}$ critical values of roll rate corresponding to $\bar{q}$ values $\bar{q}_1$ and $\bar{q}_2$ where $p^*_{s,1} < p^*_{s,2}$, deg/sec or rad/sec

p airplane roll rate about X body axis, deg/sec or rad/sec

p_s stability-axis roll rate, deg/sec or rad/sec

$\dot{p}_{ARI}$ roll angular acceleration due to ARI, deg/sec^2 or rad/sec^2

q airplane pitch rate about Y body axis, deg/sec or rad/sec

$\bar{q}$ free-stream dynamic pressure, N/m^2 (lb/ft^2)

$\bar{q}_1, \bar{q}_2$	specific values of $\bar{q}$ where $\bar{q}_1 < \bar{q}_2$
r	airplane yaw rate about Z body axis, deg/sec or rad/sec
r_s	stability-axis yaw rate, deg/sec or rad/sec
$\dot{r}_{ARI}$	yaw angular acceleration due to ARI, deg/sec^2 or rad/sec^2
S	wing area, m^2 (ft^2)
t	time, sec
$t_{1/2}$	time to damp to one-half amplitude, sec
u,v,w	components of airplane velocity along X, Y, and Z body axes, m/sec (ft/sec)
V	airplane resultant velocity, m/sec (ft/sec)
X,Y,Z	airplane body axes (see fig. 1)
α	angle of attack, deg
β	angle of sideslip, deg
δ_a	aileron deflection, positive for left aileron deflected with trailing edge up, deg
δ_{ARI}	combined yaw and roll-control deflections obtained by ARI, deg
δ_d	differential horizontal-tail deflection, positive for left tail deflected with trailing edge up, deg
δ_h	horizontal-tail deflection, positive for tail deflected with trailing edge down, deg
δ_{ls}	lateral stick deflection, positive for right roll command, cm (in.)
δ_{ped}	rudder pedal deflection, positive for right yaw command, cm (in.)

δ_r rudder deflection, positive for rudder surface deflected with trailing edge left, deg

θ, ϕ, ψ Euler angles, deg

ρ air density, kg/m^3 ($slugs/ft^3$)

Ω total airplane angular rate vector, deg/sec

Stability derivatives:

$$C_{l_p} = \frac{\partial C_l}{\partial \frac{pb}{2V}} \qquad C_{l_r} = \frac{\partial C_l}{\partial \frac{rb}{2V}} \qquad C_{l_\beta} = \frac{\partial C_l}{\partial \beta} \qquad C_{l_{\delta_d}} = \frac{\partial C_l}{\partial \delta_d} \qquad C_{l_{\delta_a}} = \frac{\partial C_l}{\partial \delta_a}$$

$$C_{l_{\delta_r}} = \frac{\partial C_l}{\partial \delta_r} \qquad C_{l_{\delta_{ARI}}} = \frac{\partial C_l}{\partial \delta_{ARI}} \qquad C_{l_{\dot{\beta}}} = \frac{\partial C_l}{\partial \frac{\dot{\beta} b}{2V}} \qquad C_{n_p} = \frac{\partial C_n}{\partial \frac{pb}{2V}}$$

$$C_{n_r} = \frac{\partial C_n}{\partial \frac{rb}{2V}} \qquad C_{n_\beta} = \frac{\partial C_n}{\partial \beta} \qquad C_{n_{\beta,dyn}} = C_{n_\beta} \cos \alpha - \frac{I_Z}{I_X} C_{l_\beta} \sin \alpha$$

$$C_{n_{\delta_r}} = \frac{\partial C_n}{\partial \delta_r} \qquad C_{n_{\delta_d}} = \frac{\partial C_n}{\partial \delta_d} \qquad C_{n_{\delta_a}} = \frac{\partial C_n}{\partial \delta_a} \qquad C_{n_{\delta_{ARI}}} = \frac{\partial C_n}{\partial \delta_{ARI}}$$

$$C_{n_{\dot{\beta}}} = \frac{\partial C_n}{\partial \frac{\dot{\beta} b}{2V}} \qquad C_{Y_\beta} = \frac{\partial C_Y}{\partial \beta}$$

Subscripts:

aug augmented

crit critical

DR Dutch roll

Abbreviations:

ARI	aileron-rudder interconnect
CAS	command augmentation system
CCV	control-configured vehicle
KIAS	knots indicated airspeed
LCDP	lateral control divergence parameter
LSRI	lateral-stick-to-rudder interconnect
PIO	pilot-induced oscillation
RSS	relaxed static stability

A dot over a variable denotes a derivative with respect to time.

An arrow over a variable denotes a vector.

BACKGROUND

Aerodynamic Considerations

The following discussion is provided to briefly identify some of the fundamental and important high-angle-of-attack aerodynamic characteristics that must be addressed in designing a control system for these flight conditions. It is emphasized that this summary is not intended to be a comprehensive treatment of the subject. (See ref. 1 for a more detailed overview.) The discussion of aerodynamics presented herein is limited to one set of aerodynamics which exhibits general stability and control trends that are representative of many current fighter designs. Also, the particular discussion in this section is limited to configurations designed to have inherent longitudinal static stability (not requiring artificial static stability augmentation). A subsequent section of this paper, "Future Concepts and Applications," addresses airplane configurations employing control-configured-vehicle (CCV) concepts wherein the airframe is purposely designed to have low or negative static longitudinal stability. It is believed that analysis of such representative characteristics provides a very useful illustration of the effects of various

control-system design features. This paper is not intended to be an analysis of the particular problems of any one specific airplane design.

Shown in figure 2 are low-speed wind-tunnel lift and pitching-moment data for the subject airplane with neutral controls. The lift curve is nearly linear up to $\alpha = 15^{\circ}$, where a change in slope indicates progressive stall of the outer wing. Note that maximum lift does not occur until about $\alpha = 30^{\circ}$, so that the desire for maximum maneuverability dictates the need to be able to fly safely and effectively up to this angle of attack. The pitching-moment curve shows satisfactory levels of stability at high angles of attack. In general, longitudinal stability at high angles of attack is not a significant problem for the current generation of fighter aircraft except those that employ CCV concepts wherein the airframe is purposely designed to exhibit low or negative aerodynamic stability. The problem may be more severe, however, for future designs, particularly those with highly swept wings designed for supersonic maneuverability. The impact of CCV concepts on high-angle-of-attack pitch control is addressed in a subsequent section of this paper.

The variation of static lateral-directional stability with α for the airplane is shown in figure 3 for two values of Mach number, 0.15 and 0.9. The low-speed data indicate a rapid degradation in directional stability above $\alpha = 10^{\circ}$ such that C_{n_β} is zero at $\alpha \approx 16^{\circ}$ and exhibits highly unstable values at higher angles of attack. The reduction of C_{n_β} and marked changes to be discussed for other stability derivatives are results of aerodynamic interference caused by stalled and vortex flow. Lateral stability C_{l_β} is maintained at a high level with increasing angle of attack such that the airplane is dynamically stable throughout the angle-of-attack range as indicated by the $C_{n_{\beta,dyn}}$ parameter. The $C_{n_{\beta,dyn}}$ parameter has been used in past investigations an an indication of the existence of directional divergence ("nose slice") at high angles of attack. Negative values of this parameter usually indicate the existence of a divergence. The data presented for $M = 0.9$ show that both the lateral and the directional stability can be noticeably degraded at transonic Mach numbers. At $M = 0.9$, C_{n_β} is negative above $\alpha = 13^{\circ}$, and C_{l_β} values are significantly less stable than those exhibited by the configuration at low Mach number. Near $\alpha = 20^{\circ}$, the stability characteristics have degraded to the point that $C_{n_{\beta,dyn}}$ is negative, which indicates the possibility of a divergence.

Turning to lateral-directional control characteristics, rudder effectiveness is plotted versus angle of attack in figure 4. At low speeds, the data show a rapid reduction in $C_{n_{\delta_r}}$ above $\alpha = 20^{\circ}$, such that the rudder is completely ineffective by $\alpha = 40^{\circ}$.

Comparison with the $M = 0.9$ data indicates significantly lower rudder effectiveness at the high-speed condition. These characteristics indicate that it would be difficult to maneuver the airplane effectively by using the rudder above $\alpha \approx 30^{\circ}$ because of the lack of yaw control.

Figure 5 shows the rolling- and yawing-moment derivatives due to differential deflection of the horizontal stabilators used for roll control on the subject configuration. The low-speed data at $M = 0.15$ indicate that the rolling-moment effectiveness of these controls is maintained to high angles of attack and that proverse yawing moment is produced up to $\alpha = 32^{\circ}$. The transonic data presented for $M = 0.9$ shows a degradation in these characteristics with a marked reduction in rolling-moment derivative $C_{l_{\delta_d}}$ above $\alpha = 20^{\circ}$ and a change of yawing-moment derivative $C_{n_{\delta_d}}$ from proverse to adverse at significantly lower angles of attack. The overall roll effectiveness of the airplane can be appraised by using the lateral control divergence parameter (LCDP), which is defined as

$$\text{LCDP} = C_{n_\beta} - C_{l_\beta} \frac{C_{n_{\delta_d}}}{C_{l_{\delta_d}}}$$

A negative value of this parameter is indicative of roll reversal. When a roll reversal is encountered, a right roll-control input by the pilot will cause the airplane to roll to the left. Computed values of LCDP for the subject airplane are shown in figure 6. The results for $M = 0.15$ indicate that reversed response will be encountered above $\alpha = 22^{\circ}$, due primarily to the high level of static directional instability discussed previously. The degraded stability and control characteristics at $M = 0.9$ are reflected in the LCDP values, which predict that reversed response will occur above $\alpha = 16^{\circ}$. These results indicate the importance of considering Mach number effects in designing a control system for these flight conditions.

The dynamic derivatives produced by rolling, yawing, and pitching are also important parameters in high-angle-of-attack flight dynamics and must certainly be accounted for in the control-system design process. Unfortunately, these derivatives are not as readily obtainable as the static stability data discussed previously. Figure 7 shows the variation with angle of attack of the roll and yaw damping derivatives for the subject configuration measured during low-speed wind-tunnel forced-oscillation tests. The yaw-damping data show that the level of damping is maintained with increasing angle of attack up to and beyond maximum lift. Roll damping, on the other hand, experiences a sharp

reduction above $\alpha \approx 10^{o}$ due to progressive wing stall. The low values of roll damping for $\alpha \geqq 20^{o}$ results in a poorly damped Dutch roll which degrades tracking performance. In situations such as this, designing the control system to alleviate the problem is an attractive potential solution.

Kinematic and Inertia Coupling Considerations

Coupling resulting from kinematic and inertia effects are important in varying degrees to the high-angle-of-attack flight dynamics of all modern fighter aircraft. The following discussion is a brief review of several of these phenomena that are particularly significant to the control-system design process.

Figure 8 illustrates the kinematic coupling between angle of attack and angle of sideslip that occurs when an airplane is rolled about its longitudinal axis, or X-axis, at high angles of attack. If the airplane is flying at angle of attack with the wings level and the pilot initiates a pure rolling motion about the airplane X-axis, all the initial angle of attack will have been converted into sideslip after 90^{o} of roll. Because it is undesirable to generate large amounts of sideslip at high angles of attack from a roll-performance as well as a departure-susceptibility viewpoint, most current fighters are designed to roll more nearly about the velocity vector than the body axis. It is obvious that this conical rotational motion (indicated by p_s) eliminates the coupling between α and β. Resolving p_s into the body-axis system shows that this motion involves body-axis yaw rate as well as roll rate and that these rates are related by the expression $r = p \tan \alpha$. If this equality is not satisfied during a roll, sideslip is generated as a result of kinematic coupling with $\dot{\beta}$ varying as $\dot{\beta} \approx p \sin \alpha - r \cos \alpha$.

In the case of rolling with an initial sideslip, it is seen from figure 8 that body-axis rolling results in the initial sideslip being converted into angle of attack after 90^{o} of roll with $\dot{\alpha}$ varying as $\dot{\alpha} \approx q - p \cos \alpha \tan \beta$. The second term of this expression indicates that rolling with adverse sideslip (p and β having the same signs) tends to reduce α, whereas rolling with proverse sideslip (p and β having opposite signs) tends to increase α. This latter effect can be an important consideration in that substantial increases in α can be generated as a result of kinematic coupling if the airplane is rolled with proverse β (using excessive rudder for example).

The second form of coupling important to the high-angle-of-attack dynamics of modern fighter aircraft is a result of inertial effects. Figure 9(a) illustrates the well-known inertial pitching moment that is produced when a typically fuselage-heavy fighter airplane is rolled about its velocity vector at high angles of attack. The desirability of this type of roll from the viewpoint of kinematic coupling was discussed previously; however, the nose-up pitching moment caused by inertia coupling can also be an important consideration. As an aid in visualizing this effect, the fuselage-heavy mass distribution

of the airplane is represented as a dumbbell with the mass concentrated at the two ends. If the airplane rolls about its velocity vector, the dumbbell tends to pitch up to align itself perpendicular to the rotation vector p_s. This pitching moment due to inertia coupling M_{ic} can be expressed as

$$M_{ic} = \left(I_Z - I_X\right)pr$$

Substituting

$$p = p_s \cos \alpha$$

and

$$r = p_s \sin \alpha$$

gives

$$M_{ic} = \left(I_Z - I_X\right)p_s^2 \cos \alpha \sin \alpha = \frac{1}{2}\left(I_Z - I_X\right)p_s^2 \sin 2\alpha$$

The previous expression shows that the inertia-coupling pitching moment resulting from stability-axis rolling is always positive (nose up) for positive angle of attack, increases with increasing angle of attack, and varies as the square of the roll rate. Thus, if high rates of roll can be generated at high angles of attack, significant nose-up moments are produced which cause uncommanded increases in angle of attack and, if longitudinal stability is low, can lead to loss of control.

The inertia-coupling yawing moment which results from the combination of roll and pitch rates is illustrated in figure 9(b). The airplane mass distribution is represented by the dumbbell and the airplane is shown rolling to the right and pitching up. As can be seen, the dumbbell tends to yaw nose-left to align itself perpendicular to the rotation vector $\vec{\Omega}$. Thus, the airplane would be rolling and yawing in opposite directions. Recalling that to minimize adverse sideslip due to kinematic coupling r must be equal to $p \tan \alpha$, it is seen that this form of coupling can contribute to the buildup of large amounts of adverse sideslip which in turn can result in loss of lateral-directional control at high angles of attack.

The discussion in this section is an attempt to briefly highlight some aerodynamic, kinematic, and inertial phenomena important to the high-angle-of-attack flight dynamics of modern fighter aircraft. These phenomena must therefore be addressed in designing the control system if it is to be used to enhance departure/spin resistance. When these

considerations are not included in the design process, the resulting system can often have detrimental effects on departure/spin resistance. Examples of this are covered in the following section, which is a discussion of the effects of conventional stability augmentation systems not specifically designed for high-angle-of-attack flight conditions.

EFFECTS OF CONVENTIONAL CONTROL SYSTEMS AT HIGH ANGLES OF ATTACK

Pitch Damper

As discussed previously, current fighters designed to have a satisfactory level of static longitudinal stability at low angles of attack do not generally experience significant degradation of these characteristics with increasing angle of attack. Furthermore, conventional pitch dampers are normally designed with relatively low gains and very limited authority; therefore, such systems generally do not significantly affect departure/spin characteristics.

Yaw Damper

Yaw dampers designed to augment Dutch roll damping at low-angle-of-attack flight conditions are usually implemented by feeding aircraft yaw rate through a washout (high-pass) filter to drive the yaw control within some prescribed authority limit. At low speeds, the ability of the yaw damper to enhance Dutch roll damping tends to decrease with increasing angle of attack for several reasons. As discussed previously, the combination of low dynamic pressure and the tendency toward loss of rudder effectiveness at high angles of attack is certainly a contributing factor. However, an equally important effect, discussed in the previous section, is the decrease in static directional stability with increasing angle of attack. This reduction in C_{n_β} combined with sustained C_{l_β} causes the Dutch roll mode to become a rolling oscillation about the longitudinal body axis with little yaw rate involved. As a result, increasing the effective C_{n_r} has little impact on the Dutch roll motion at these conditions. However, in the extreme condition where C_{n_β} and C_{l_β} are degraded to the point that the airplane exhibits a yaw departure (nose slice), the damper is beneficial in that it opposes the motion and, therefore, slows the rate of divergence. This effect is generally small at low speeds because of the lack of rudder power at low values of $\bar{q}$. At higher speeds, however, the beneficial effect of the damper can be stronger.

Figure 10 is a summary of the effects of a yaw damper applied to the fighter configuration discussed in the previous section. Damping of the Dutch roll mode is computed

for 1g trim (low speed) and $M = 0.9$ and is expressed in terms of the parameter $1/t_{1/2}$. The low-speed results for the basic airplane show a decrease in damping with increasing angle of attack such that the mode is undamped (unstable) for α above about 17°. Addition of the yaw damper results in a very significant improvement in stability at the lower angles of attack; with increasing angle of attack, however, the effectiveness drops off rapidly. At $M = 0.9$, the basic airplane experiences a sharp loss in stability for $\alpha > 15^{\circ}$ because C_{n_β} becomes highly negative. By $\alpha = 20^{\circ}$, the Dutch roll mode is quite unstable, which indicates the existence of a divergence. Again, addition of the yaw damper greatly improves Dutch roll damping at the lower angles of attack. In this case, however, the effectiveness of the device does not decrease with increasing angle of attack as rapidly as in the low-speed case. At $\alpha = 20^{\circ}$, the yaw damper significantly reduces the level of instability and the resulting departure is therefore expected to be milder. This characteristic is verified in figure 11, which shows time histories of a split-S maneuver in which the airplane was maneuvered into the instability at $M = 0.9$ and $\alpha = 20^{\circ}$. The unaugmented airplane experienced a fairly rapid departure "over the top" of the turn before decelerating out of the instability region. As predicted previously, the airplane with the yaw damper active encountered a much milder uncommanded motion as it passed through the unstable area.

An additional high-angle-of-attack effect of yaw dampers is related to kinematic coupling. As discussed previously, minimization of adverse sideslip generation during rolls at high angles of attack requires that the airplane roll about the velocity vector which involves body-axis yaw rate as well as roll rate. Because the damper opposes any yaw rate, it tends to make the airplane roll about the body axis rather than the velocity vector, and thus is detrimental to roll coordination. The severity of this effect is more apparent at high-speed than at low-speed flight conditions.

Roll Damper

Conventional roll dampers are also generally designed to enhance low-angle-of-attack flying qualities – in this case to quicken the roll mode. However, the influence of the roll damper on high-angle-of-attack characteristics can be much stronger than that of the yaw damper. There are several reasons for this characteristic. One reason is that roll controls, particularly differential tail, can produce strong yawing and rolling moments at high angles of attack, whereas rudders generally tend to lose effectiveness. A second important factor is the combination of high-angle-of-attack aerodynamics and kinematics. As mentioned in the previous section, the Dutch roll mode becomes primarily a rolling motion at high angles of attack; therefore, a roll damper is more effective in stabilizing this primary lateral-directional mode of motion. Some further insight into this phenomenon can be gained by examining an expression for the damping of the Dutch

roll. In reference 2, an approximation for the damping index of this mode is developed and, with some manipulation, the damping can be expressed in terms of the parameter $1/t_{1/2}$ as follows:

$$\left(1/t_{1/2}\right)_{DR} \approx (-0.722)\left(\left(\frac{\rho SV}{m}\right)\left\{C_{Y_\beta} + \frac{mb^2}{4}\left[C_{n_\beta}\left(\frac{C_{n_r}}{I_Z}\cos\alpha - \frac{C_{l_r}}{I_X}\sin\alpha\right)\right.\right.\right.$$

$$\left.\left.\left. + \frac{I_Z}{I_X}C_{l_\beta}\left(\frac{C_{n_p}}{I_Z}\cos\alpha - \frac{C_{l_p}}{I_X}\sin\alpha\right)\right]\middle/ C_{n_{\beta,dyn}}\right\}\right.$$

$$\left. - \frac{g}{V}\left(C_{n_\beta}\sin\theta + \frac{I_Z}{I_X}C_{l_\beta}\cos\theta\cos\phi\right)\middle/ C_{n_{\beta,dyn}}\right)$$

An indication of the variation of damping with roll damping is obtained by taking the derivative of the above expression with respect to C_{l_p}:

$$\frac{\partial\left(1/t_{1/2}\right)_{DR}}{\partial C_{l_p}} \approx (0.722)\left(\frac{\rho SVb^2}{4}\right)\left(\frac{I_Z}{I_X{}^2}C_{l_\beta}\sin\alpha\right)\middle/ C_{n_{\beta,dyn}}$$

For a stable configuration $C_{n_{\beta,dyn}} > 0$, this expression shows that the sensitivity of Dutch roll damping to C_{l_p} increases with angle of attack and varies with the level of dihedral effect. Higher dihedral effect results in a greater increase in Dutch roll damping due to increased roll damping. This result substantiates the intuitive explanation given earlier that high levels of dihedral effect at high angles of attack tend to make the Dutch roll more of a rolling oscillation and, therefore, increasing roll damping would be expected to be effective in damping the mode. Thus, under these conditions, a roll damper designed for low angle of attack to augment the roll mode damping with little effect on Dutch roll damping tends to have the opposite effect at higher angles of attack.

Of course, the effect of the roll damper on high-angle-of-attack Dutch roll stability is directly related to the system gain (surface deflection per unit roll rate), which is generally low. The upper portion of figure 12 illustrates this effect for the example

fighter configuration. As discussed previously, at low speeds the airplane exhibits an undamped Dutch roll mode above $\alpha = 17^{o}$ due to loss of C_{l_p} and C_{n_β}, while C_{l_β} remains high. The oscillation is almost entirely about the roll axis and the term "wing rock" is often used to describe this type of motion. As predicted, addition of a roll damper designed for the airplane has very little effect on the Dutch roll damping at low angles of attack. The beneficial effect at higher angles of attack is evident; however, the improvement in damping is small because of the low gain of the system. When the gain is quadrupled, however, the data show that the damping above $\alpha = 10^{o}$ is greatly augmented, to the extent that the wing-rock tendency is eliminated.

Although roll dampers can have a stabilizing effect at high angles of attack if $C_{n_{\beta,dyn}}$ indicates good stability and dihedral effect is high, experience has shown that their effect can become quite the opposite as the basic airframe stability becomes marginally stable or unstable $\left(C_{n_{\beta,dyn}} \text{ low or negative}\right)$. This characteristic is also indicated by the preceding expression for $\partial\left(1/t_{1/2}\right)_{DR}/\partial C_{l_p}$, which shows that if $C_{n_{\beta,dyn}} < 0$ while dihedral effect is maintained, increasing roll damping is destabilizing. The lower portion of figure 12 illustrates this effect; values of Dutch roll damping are shown for the example airplane at $M = 0.9$. It is seen that at $\alpha = 15^{o}$ (where the configuration is stable), the roll damper enhances stability. However, at $\alpha = 20^{o}$, where the basic airplane experiences a moderate instability due to a marked loss of static directional stability, the data show that the roll damper, even with its low gain, significantly aggravates the instability. Time histories of split-S excursions through this region with and without the roll damper are shown in figure 13. As shown previously, the basic airplane experiences a moderate departure. Addition of the roll damper, however, results in a much more severe and prolonged loss of control.

The detrimental effects of a roll damper are further aggravated if the driven roll control exhibits adverse yaw. For example, if a departure to the right occurs, the damper applies left roll control which, due to its adverse characteristic, produces additional nose-right yawing moment to drive the departure.

Because of their potential for strong adverse effects at high angles of attack, most conventional roll dampers not designed for these conditions are simply deactivated at high angles of attack. Systems that employ high-gain roll dampers to correct specific high-angle-of-attack deficiencies such as wing rock should also incorporate safeguards that allow the dampers to operate when their effects are beneficial and to deactivate when their effects are detrimental to stability and departure resistance.

EFFECTS OF PITCH AND ROLL COMMAND AUGMENTATION SYSTEMS

Many current and evolving fighter designs use control laws which are more sophisticated than simple stability augmentation systems. These concepts, often referred to as maneuver-demand, or command augmentation systems (CAS), are designed to provide the pilot with airplane response characteristics that remain relatively constant over a large flight envelope. The behavior of an airplane with these control laws can be quite different from that of an airplane using more conventional direct stick-to-surface control. For example, airplanes using such CAS concepts are usually equipped with a control logic so that a given stick force (or deflection) commands a specific response, such as specified pitch or roll rates and/or normal acceleration response. In a typical pitch CAS (fig. 14), a mixture of pitch rate and normal acceleration is commanded proportional to pilot stick position (or force) to provide a uniform pitch response over a wide angle-of-attack and speed envelope. However, with such a response-command system, for any nonaccelerated flight condition, the stick must be in a neutral position. Whenever the stick is held aft of neutral, the pilot is commanding an accelerated flight condition as opposed to commanding a particular trim angle of attack (which would be the case in an airplane with conventional augmentation). For example, at a fixed power setting (thrust level), consider a pilot rolling such an airplane into a turn, applying a fixed partial aft stick deflection (or force), and holding this control input. If the pilot is commanding an accelerated condition that cannot be sustained with available thrust, the airspeed decreases and the pitch control system commands increasing angle of attack in an attempt to maintain the commanded pitch rate and normal acceleration. If such a system is not authority limited or angle-of-attack limited, the pitch CAS eventually commands a full pitch-control deflection and increases the airplane angle of attack to the maximum trim angle of attack, usually an angle of attack at or beyond maximum lift. This characteristic is illustrated in the time histories shown in figure 15; in this maneuver, the pilot banked the airplane into a turn and applied a step stick input (commanding normal acceleration and pitch rate) near $t = 8$ sec, establishing an initial angle of attack of 14°. Thereafter, the stick position and power setting were held constant. As the airplane decelerated, the angle of attack increased to over 35° as the pitch-control system attempted to maintain the commanded pitch rate and normal acceleration. Such behavior can lead to inadvertent stall entries if the pilot is unaware of this control-system characteristic. Moreover, if the airplane exhibits degraded lateral/directional stability and control in the stall, inadvertent loss of control and spin entry may occur.

With regard to the lateral axis, the CAS concept can be used to provide a uniform roll response to lateral stick inputs over a wide range of flight conditions. With this characteristic, as the aileron rolling moment becomes lower because of either lower dynamic pressure or reduced control effectiveness, the control system (CAS) drives the

control surfaces to larger deflections in seeking to provide the commanded roll rate. Consider, for example, an airplane flying in a decelerating windup turn to track a target airplane. As the maneuver progresses, the airspeed steadily decreases while the angle of attack is increased to maintain the desired turn rate. As the pilot attempts to track the target airplane, the aileron deflections increase significantly as the CAS attempts to maintain the constant roll-rate response. If the airplane control system incorporates a roll/yaw interconnect, which deflects the rudders in proportion to aileron deflection for coordination, rudder deflections also increase markedly as the maneuver progresses into the low-speed, high-angle-of-attack regime. As with the pitch CAS described previously, the pilot is often unaware that such large control deflections are occurring. When the lateral-directional stability of the airplane is low, as is often the case near maximum lift, such large-amplitude directional control (rudder) deflections can excite oscillations which may degrade fine tracking at high angles of attack.

Another potential adverse characteristic of a roll-rate CAS at high angles of attack arises when the pilot attempts to roll the airplane using only the rudder pedals. The practice of rolling with rudder-pedal inputs is a very common technique in many current fighters where roll response to lateral stick inputs is either low or reversed from the desired direction. In such airplanes, the pilot applies rudder to generate proverse sideslip which produces the desired rolling moment via the dihedral effect of the airplane $\left(\text{assuming } C_{l_\beta} \text{ is sufficiently stable}\right)$. In this case, when the lateral stick is kept centered (neutral), the roll CAS causes the ailerons to oppose the roll rate generated by the rudders. This CAS response is similar to that of a conventional roll damper system, except more dramatic in that roll CAS systems are often high-gain, full-authority as opposed to low-gain, very limited-authority roll dampers. An example of such a response is shown in figure 16 which shows a roll-reversal attempt using only rudder inputs during a pull-up maneuver. At $t \approx 6$ sec and $\alpha \approx 15^\circ$, the pilot applied full left rudder while keeping the lateral stick neutral. Although about 7° of steady-state sideslip was generated, the roll response was comparatively slow because the roll-rate CAS applied over 20° of opposite aileron deflection in countering the uncommanded roll rate. In the extreme situation, attempting to roll such an airplane at high angles of attack with rudder pedals can result in the inadvertent application of nearly full "cross controls" (roll control opposite to rudder), which is a prospin control input for most current fighter airplanes. For conventional airplane designs, it is quite common for the pilot to use the rudder alone for roll control at high angles of attack; therefore, most pilots tend to use rudders instinctively for roll control at high angles of attack. Consequently, when pilots are transitioned into airplanes using the CAS concepts, training is required to insure that the pilot fully understands the important differences in airplane response to controls for the CAS type airplane. With a properly designed roll CAS, the pilot can roll the airplane

over a large angle-of-attack range using conventional lateral-stick inputs. The pilot should not attempt to roll the airplane using only rudder pedals since the roll CAS opposes the roll rate and degraded roll performance results.

HIGH-ANGLE-OF-ATTACK CONTROL CONCEPTS

Within the last decade, there has been increasing emphasis on including the foregoing high-angle-of-attack considerations in the control-system design process for fighter aircraft. As a result, a number of high-angle-of-attack control concepts have emerged, many of which are now being very effectively used in the latest fighters (refs. 3 to 6). These concepts include roll- and yaw-control interconnects, stability-axis yaw damping, static stability augmentation, angle-of-attack limiting, and automatic spin prevention.

Roll- and Yaw-Control Interconnects

The basic rationale for roll/yaw interconnect systems, often called aileron-rudder interconnect (ARI), arise from the high-angle-of-attack kinematic coupling phenomenon discussed previously. Recalling that avoidance of large slideslip generation during high-angle-of-attack rolls requires body-axis yawing as well as rolling, it is seen that the proper response to pilot roll inputs is an appropriate mixture of yaw- and roll-control deflections. Furthermore, because the required relationship between yaw and roll rates is $r = p \tan \alpha$, the needed ratio of yaw to roll control increases with increasing angle of attack. An additional factor that must be taken into account is the yawing moment produced by the roll control. As discussed in the section on aerodynamic considerations, the general trend with increasing angle of attack is toward adverse yaw. For situations where the adverse yaw due to roll control is significant, the interconnect gain must be sufficiently high to provide enough rudder deflection to both counter the adverse yaw and to minimize kinematic coupling. This factor is best summarized by using the lateral control divergence parameter (LCDP), which, in the presence of an interconnect system, is given by

$$\mathrm{LCDP} = C_{n_\beta} - C_{l_\beta}\left(\frac{C_{n_{\delta_a}} + KC_{n_{\delta_r}}}{C_{l_{\delta_a}} + KC_{l_{\delta_r}}}\right)$$

where K is the gearing ratio between the yaw and roll controls.

Returning to the example fighter configuration, figure 17 shows computed values of LCDP for the airplane with and without an optimized ARI system. As shown previously, the basic configuration exhibits negative values of LCDP, which indicates susceptibility to control-induced departures because of improper response to pilot roll commands. Addition of the ARI results in large positive values of LCDP throughout the angle-of-attack range, which indicates normal roll response and high resistance to control-induced departures.

ARI systems are generally implemented in one of two methods. The first method involves driving the rudders directly proportional to roll-control deflection, which results in a true aileron-rudder interconnect. In the second implementation, the rudders are driven by pilot lateral-stick deflection, so that it would be more accurate to refer to such a system as a lateral-stick-to-rudder interconnect (LSRI). The true ARI has an advantage over the LSRI in that with the former the rudder is driven by roll-control deflection so that it can more accurately compensate for the characteristics of these controls. Nevertheless, the LSRI implementation is often used in situations where, in addition to bringing in the rudder, it is also necessary to fade out roll-control deflection with increasing angle of attack because of excessive adverse yaw or insufficient rudder effectiveness.

In summary, ARI systems can provide several very significant improvements at high angles of attack. The first is the proper coordination of high-angle-of-attack rolls, which thereby inhibits departures due to improper roll response as discussed previously. A second benefit which results directly from the improved coordination is the enhancement of roll performance as illustrated in figure 18. Peak roll rates are plotted versus angle of attack. These rates are obtained for full lateral-stick inputs applied during turns at $M = 0.6$ and $h = 9144$ m (30 000 ft). The airplane was equipped with an ARI system and data were obtained with and without the system active. As can be seen, the basic airplane exhibited a sharp drop in roll performance with increasing angle of attack primarily because of low static directional stability. Above $\alpha = 21^{\circ}$, roll reversal was encountered. Activation of the ARI resulted in much improved roll performance throughout the angle-of-attack range and the roll-reversal characteristic was eliminated.

An additional important benefit of the ARI is that it greatly simplifies the pilot work load at high angles of attack. Without the ARI, the pilot must properly coordinate the rolls himself, which is a very difficult task, particularly in the air combat environment involving rapid, vigorous maneuvering with the pilot's attention out of the cockpit. As a result of the high work load, coordination is often poor and results in the degraded roll performance and departure susceptibility problems discussed previously. With an ARI system, the coordination task is automatically performed by the control system so that the pilot can use the same technique to roll the airplane at all angles of attack.

This significantly reduces the pilot work load and enhances the ability to maneuver the airplane effectively.

Because an ARI system automatically applies coordinating rudder in the direction of the stick input, it inhibits the pilot from obtaining cross controls (yaw and roll controls in opposite directions) which are departure and spin inducing. Thus, an additional benefit provided by an ARI is that it prevents the departure caused by inadvertent pilot application of cross controls.

Despite the many enhancing features of ARI systems, there are also some potential problem areas that should be kept in mind in designing these systems. An important example is a case in which the airplane exhibits very poor Dutch roll damping characteristics, such as the wing-rock phenomenon discussed previously. In this example, the addition of ARI (particularly if the system gain is too high) can lead to aggravation of the oscillation in the form of divergent lateral pilot-induced oscillation (PIO). Some insight into this phenomenon can be gained by considering the pilot as a simple roll damper trying to damp the wing-rock motion. Thus, the roll inputs of the pilot are in a direction which opposes the roll rate, which, as was discussed previously, is the primary angular motion seen in this type of oscillation. The rolling moments resulting from the pilot inputs would thus augment C_{l_p}, which is stabilizing; however, the yawing moments obtained through ARI produce a negative increment in C_{n_p}, which is destabilizing. If the ARI gain is high enough that the adverse effect of C_{n_p} is stronger than the stabilizing effect of C_{l_p}, the net result is an aggravation of the low damping condition.

An indication of the maximum ARI gain above which closed-loop instability can occur is obtained by reexamining the approximation for the damping of the Dutch roll mode shown earlier. The pilot is modeled as a simple roll damper with a gain of K_p degrees of control deflection per deg/sec of roll rate. Consider the combined yaw- and roll-control deflections obtained through the ARI as a single control deflection δ_{ARI} with the resulting derivatives $C_{l_{\delta_{ARI}}}$ and $C_{n_{\delta_{ARI}}}$. As discussed previously, the effect of the pilot closing the loop as a roll damper is equivalent to modifying C_{l_p} and C_{n_p} with the increments given by

$$\Delta C_{l_p} = \frac{2V}{b}\left(C_{l_{\delta_{ARI}}}\right)K_p$$

$$\Delta C_{n_p} = \frac{2V}{b}\left(C_{n_{\delta_{ARI}}}\right)K_p$$

Adding these increments into the approximation of the Dutch roll damping parameter $\left(1/t_{1/2}\right)_{DR}$ shown previously and taking the derivative of that expression with respect to K_p gives

$$\frac{\partial\left(1/t_{1/2}\right)_{DR}}{\partial K_p} \approx (-0.722)(\bar{q}Sb)\left(\frac{I_Z}{I_X} C_{l_\beta}\right)\left(\frac{C_{n_{\delta_{ARI}}}}{I_Z} \cos\alpha - \frac{C_{l_{\delta_{ARI}}}}{I_X} \sin\alpha\right) \Big/ C_{n_{\beta,dyn}}$$

For the conditions $C_{n_{\beta,dyn}} > 0$ and $C_{l_\beta} < 0$, the effect of the pilot closing the loop with an ARI system is stabilizing if

$$\frac{C_{n_{\delta_{ARI}}}}{I_Z} \cos\alpha - \frac{C_{l_{\delta_{ARI}}}}{I_X} \sin\alpha > 0$$

or

$$\frac{C_{n_{\delta_{ARI}}}}{I_Z} \cos\alpha > \frac{C_{l_{\delta_{ARI}}}}{I_X} \sin\alpha$$

By convention, $C_{l_{\delta_{ARI}}}$ and $C_{n_{\delta_{ARI}}}$ are negative, so the above expression can be written as

$$\frac{\left|C_{n_{\delta_{ARI}}}\right|}{I_Z} \cos\alpha < \frac{\left|C_{l_{\delta_{ARI}}}\right|}{I_X} \sin\alpha$$

Multiplying both sides by $\bar{q}Sb\left|\delta_{ARI}\right|$ yields

$$\left(\frac{\bar{q}Sb\left|\delta_{ARI}\right|\left|C_{n_{\delta_{ARI}}}\right|}{I_Z}\right) < \left(\frac{\bar{q}Sb\left|\delta_{ARI}\right|\left|C_{l_{\delta_{ARI}}}\right|}{I_X}\right) \tan\alpha$$

The two terms in parentheses in the preceding expression are simply the yaw and roll angular accelerations caused by δ_{ARI}, so that the requirement for enhancement

of closed-loop stability is simply

$$\left|\dot{r}_{ARI}\right| < \left|\dot{p}_{ARI}\right| \tan \alpha$$

Recalling that proper roll coordination at high angles of attack requires roll about the velocity vector with $r = p \tan \alpha$, the preceding inequality states that in order that the ARI not degrade closed-loop stability, its gain must not be so high as to overcoordinate the roll. Thus, from the viewpoint of closed-loop stability, it is desirable to design an ARI such that some adverse sideslip is generated during stick rolls at high angles of attack. More specifically, it is important to avoid excessive ARI gains which result in overcoordination which generates proverse sideslip, especially if the airplane exhibits low inherent damping.

An example of the potential adverse effect of ARI systems on closed-loop stability is contained in figure 19. The time histories, which were obtained in a piloted simulation study, are indicative of piloted attempts to track a target airplane performing a steady windup turn. The study airplane exhibited wing rock at angles of attack greater than 17°. The time histories on the left-hand side of the figure show the performance obtained with a properly configured ARI system designed with the aforementioned considerations in mind. It is seen that as the pilot pulled to about $\alpha = 20^{\circ}$, the airplane exhibited a relatively modest amplitude wing-rock motion. However, there was no tendency toward PIO, and the pilot stated that the oscillations did not significantly degrade tracking performance. The maneuver was repeated with the ARI gain doubled such that stick rolls were overcoordinated with significant generation of proverse sideslip. The time histories on the right-hand side of figure 19 show that a rapidly divergent PIO occurred as the pilot pulled into the wing-rock region. After three oscillation cycles, the pilot realized that he was driving the instability and centered the stick. The oscillation amplitude immediately decreased, which verified that the divergence was in fact a PIO caused by the excessive ARI gain.

The preceding results illustrate the importance of proper tailoring of an ARI system to the particular characteristics of the airplane and identify another consideration that should be addressed in the design process. As discussed previously in the section on aerodynamic considerations, the high-angle-of-attack stability and control characteristics of modern fighter aircraft often vary significantly with Mach number. To properly account for these effects, it may be necessary to include Mach number as a scheduling parameter in the ARI design. If this is not done, the design is compromised, which not only results in degraded system effectiveness but may also lead to the closed-loop stability problem discussed previously.

Another potential disadvantage of ARI systems results from the fact that they do not allow full cross controls to be applied. As discussed previously, this is beneficial in preventing inadvertent application of such controls which can result in departures. However, if a departure or spin entry should occur, the optimum spin recovery procedures for modern fighter aircraft involves maximum cross controls (roll control with and yaw control against the rotation rate). For this reason, the design of an ARI system should include the capability to deactivate the system or some other provision for allowing the application of full recovery controls in the event of a spin entry.

Two other potential problem areas arising from the use of ARI systems should be briefly mentioned. The first is associated with the nose-up inertia coupling resulting from stability-axis rolling. Because ARI systems promote this type of roll, use of such systems tends to accentuate this form of coupling. The second potential problem is that some pilot adaptation is usually required in flying an ARI-equipped airplane for the first time. The coning motion resulting from stability-axis rolling and the associated lateral acceleration at the cockpit may be disconcerting to the pilot at first. However, experience has shown that after a brief familiarization period, most pilots adapt quickly to flying with an ARI system and are able to take maximum advantage of the benefits provided by the concept.

Stability-Axis Yaw Damper

A stability-axis yaw damper is often used in conjunction with an ARI system. The combination is a logical one. The ARI applies the appropriate mix of roll and yaw controls in response to pilot inputs to make the airplane roll approximately about the velocity vector, and the stability-axis yaw damper reinforces this motion by attempting to damp out any residual r_s. As shown in figure 20, these devices are normally implemented by driving the yaw control with an approximation for stability-axis yaw rate $r_s \approx r - p\alpha$.

Many of the benefits of this concept are similar to those provided by ARI systems discussed previously and involve the advantage of stability-axis rolling – minimization of sideslip generation and the resulting improvement in roll performance. An additional benefit of the damper is that it can enhance Dutch roll damping up to high angles of attack, particularly if static stability is maintained $\left(C_{n_{\beta,dyn}} > 0\right)$. At low angles of attack, the body-axis yaw-rate component dominates and effectively augments damping. As discussed previously, body-axis dampers tend to lose effectiveness with increasing angle of attack; however, the $p\alpha$ component can maintain r_s damper effectiveness to much higher angles of attack. Figure 21 illustrates this characteristic. Computed values of $\left(1/t_{1/2}\right)_{DR}$ are plotted for the example fighter configuration with and without a stability-axis yaw-damper system. As can be seen, the damper effectively augments Dutch roll damping throughout the angle-of-attack range.

Although the stability-axis yaw damper is more beneficial than a body-axis damper under most conditions, an exception is the case in which the airplane exhibits a rolling departure caused by loss of static directional stability. As discussed in a previous section, the conventional yaw damper can significantly reduce the severity of such a departure, particularly at high-speed flight conditions. A stability-axis yaw damper would be less effective in this case because the roll-rate component $p\alpha$ would command rudder deflection in the direction of the departure and hence the net deflection to oppose the motion would be less than if only body-axis yaw rate was used.

Lateral-Directional Static Stability Augmentation

As mentioned in the discussion of aerodynamic considerations, degradation of lateral-directional dynamic stability at high angles of attack is most often due to loss of static directional stability and dihedral effect. Damper systems based on rate feedback, such as the stability-axis yaw damper, are generally less effective in augmenting stability in this situation. Obviously, the desirable solution is to directly augment C_{n_β} and C_{l_β} by driving the appropriate controls with a sideslip signal. Figure 22 shows data for a configuration which typifies the loss of dynamic stability at high angles of attack due to degraded characteristics of C_{l_β} and C_{n_β}. The loss in static stability above $\alpha = 25^\circ$ is reflected in a sharp drop in $C_{n_{\beta,dyn}}$, which indicates a possible directional divergence at $\alpha = 30^\circ$. Also shown in figure 22 are results obtained by augmenting C_{n_β} and C_{l_β} above $\alpha = 25^\circ$. The resulting values of $C_{n_{\beta,dyn}}$ remain large at high angles of attack, which indicates that there is no instability in this region. In this case, the augmentation of C_{n_β} and C_{l_β} was accomplished by feeding a β signal to drive the differential tails above $\alpha = 25^\circ$. Differential tail deflections on the particular configuration produced large adverse yawing moments at high angles of attack, such that they could not be used for rolling in this regime. These large yawing moments, however, were used to augment stability as in the following augmentation law:

$$\delta_d = K_\beta \beta \qquad \left(K_\beta > 0\right)$$

$$C_{l_{\beta,aug}} = C_{l_\beta} + K_\beta C_{l_{\delta_d}}$$

$$C_{n_{\beta,aug}} = C_{n_\beta} + K_\beta C_{n_{\delta_d}}$$

Since $C_{l_{\delta_d}}$ is negative, the feedback of β to the differential tail augmented dihedral effect. In addition, because $C_{n_{\delta_d}}$ was positive (adverse), the feedback also augmented directional stability by the increment $K_\beta C_{n_{\delta_d}}$, which was considerable since $C_{n_{\delta_d}}$ was large. Note that the simultaneous augmentation of dihedral effect and directional stability using the single control would not be possible if $C_{n_{\delta_d}}$ were not adverse. This case illustrates the important concept of using all available control moments for augmentation and control at high angles of attack, including those that are conventionally considered adverse, since these controls can often be quite powerful in the stall region.

This concept of augmenting static lateral-directional stability has not as yet been implemented and used on production aircraft primarily because of the difficulty in obtaining an accurate measurement of sideslip at high-angle-of-attack flight conditions. However, the potential benefits of this concept warrant further development.

Angle-of-Attack Limiting

The basic rationale for using an angle-of-attack limiter is illustrated in figure 23. A conceptual plot is shown of the variation of stability and control characteristics for a fighter as angle of attack increases. The characteristics are shown to degrade from departure-resistant at low angles of attack to departure-prone at high angles of attack. It should be noted that the divergence problem can be lateral-directional or longitudinal. Whatever the case, the rationale for using an angle-of-attack limiting system is to prevent the airplane from entering the departure-prone region. These systems are usually implemented by using angle of attack and filtered pitch rate (for lead) to drive the pitch control to inhibit excursions beyond the set angle-of-attack limit. Mach number scheduling is also sometimes necessary to account for Mach number effects on the aerodynamic characteristics.

The benefits provided by this concept are obvious. By preventing excursions into regions of poor departure resistance, the chances of encountering loss of control and possible spin entry are greatly reduced. Furthermore, because this is accomplished automatically by the system, the pilot's task is simplified in that he can confidently apply up to maximum nose-up command without fear of overrotating into regions of poor stability and control characteristics.

Unfortunately, the angle-of-attack limiting concept also entails some inherent drawbacks. An obvious one is that if it is necessary to set the limit significantly below the angle of attack for maximum lift, then a maneuverability penalty is incurred. Furthermore, the limiter negates the ability to perform rapid, momentary rotations to extreme

angles of attack, which can be a useful tactical maneuver. Even within the angle-of-attack envelope allowed by the limiter, nose-up pitch response, particularly near the boundary, can be sluggish because of the pitch-rate lead information used to minimize overshoot of the boundary.

A final limitation of angle-of-attack limiting systems is that they are not foolproof. Their effectiveness is of course limited by that of the pitch control through which they operate. Thus, an effective technique for defeating angle-of-attack limiter systems is to decelerate to very low airspeeds in a nose-high climb; the ensuing lack of dynamic pressure negates the ability of the limiter to prevent angle-of-attack excursions beyond the limit value. Other maneuvers that can potentially defeat the limiter system involve sustained high roll rates during which sufficient nose-up inertia coupling moments are generated to overpower the available nose-down control moment. This type of maneuver can be especially critical for fighters incorporating the CCV concept of relaxed static stability in pitch. This problem is discussed in more detail in a subsequent section of this paper.

Automatic Spin Prevention

Experience has shown that spins can be avoided if the proper recovery controls are applied as quickly as possible following loss of control. Unfortunately, during air combat the pilot's attention is occupied with many other tasks besides control of the aircraft and as a result, there is often a significant delay between occurrence of a departure and pilot response to it. Furthermore, following recognition of the out-of-control condition, the inputs applied by the pilot may not be optimum for recovery and, in the extreme case, may even aggravate the departure and accelerate the spin entry. It would appear, therefore, to be highly desirable to relegate the spin prevention task to an automatic system. A system capable of this task would have several inherent advantages over the human pilot, including (1) quicker and surer recognition of an incipient spin, (2) faster reaction time for initiation of recovery, (3) application of correct spin recovery controls, and (4) elimination of tendencies toward spin reversal. Reference 3 documents some early investigations of automatic spin-prevention systems conducted at the Langley Research Center. Simulation results and flight tests of subscale dynamic models showed that such systems could be very effective in preventing spins, even for fighter configurations that are very spin prone.

The basic implementation concept for these systems is conceptually illustrated in figure 24. Regions representing the normal maneuvering envelope (lower α and r) and the developed spin (high α and r) are shown on a yaw-rate/angle-of-attack plot. The area between these two regions indicates the departure and incipient spin phases, where the system activation threshold would be located. It is generally desirable to place the threshold as far from the developed spin region as practical to maximize system

effectiveness and speed of recovery to controlled flight. On the other hand, placement of the threshold too close to the maneuver envelope could result in the system interfering with the pilot's normal control of the airplane. Each system must therefore be tailored for the specific stall/spin characteristics of the particular configuration. Once an impending spin has been identified, the system commands controls for spin recovery which for modern, fuselage-heavy fighter airplanes normally consist of roll controls with the spin, rudder against the spin, and nose-up pitch control.

Some recent results of application of automatic spin prevention to a current fighter configuration are shown in figure 25. These results were obtained during free-flight tests of an unpowered, subscale dynamic model (additional information on this test technique is given in ref. 7). The time histories shown on the left-hand side of figure 25 were obtained for the basic configuration not equipped with a spin prevention device. The spin-entry attempt was initiated from a split-S maneuver by applying and holding full cross controls starting at $t \approx 5$ sec. The control system of this airplane incorporated a roll/yaw control interconnect which not only drove rudders with lateral-stick inputs but also reduced maximum roll-control deflections at high angles of attack. However, to make possible the application of full-recovery controls in the event of a spin, the interconnect was deactivated when yaw rate exceeded a preset value. As a result of the interconnect feature, much less than maximum prospin control deflections were obtained even though the pilot was holding full inputs. Nevertheless, yaw rate and angle of attack increased steadily. At $t \approx 12$ sec, the yaw rate exceeded the value for deactivation of the interconnect system, and full cross controls were obtained which accelerated the spin entry. Shortly thereafter, the model stabilized in a fast, flat spin. The results obtained with an automatic spin-prevention feature incorporated in the control system are shown on the right-hand side of figure 25. Although essentially the same inputs were made by the pilot, no spin entry occurred. Each time yaw rate began to increase and exceeded the activation threshold of the system ($t \approx 8$ and 12 sec), antispin controls were automatically applied which quickly reduced the rotation rate. The resulting motion can best be described as a steep spiral from which recovery was immediately obtained when the pilot inputs were neutralized.

An inherent characteristic of automatic spin-prevention systems which is potentially a cause of concern is the high control authority that is generally required for maximum effectiveness. This means that upon activation they necessarily take some if not all control away from the pilot. Under nominal conditions, this is a satisfactory situation; however, the implications under a failure condition are more serious. For example, if a malfunction in the system causes it to activate when the airplane is in fact within its normal maneuver envelope, the control action caused by the system could drive the airplane into a spin without the pilot being able to prevent it. Reliability is, therefore, a critical factor in the design of these systems.

In concluding this discussion of automatic spin prevention, a comment should be made regarding the effectiveness of this concept compared with departure prevention. Experience has shown that although spin-prevention systems are desirable from a safety viewpoint, much greater improvements in tactical effectiveness would be expected with systems that prevent departures rather than allowing them to occur. However, departure-prevention control schemes are often incompatible with the requirements for spin prevention and recovery. An example mentioned previously is the inability to obtain optimum spin-recovery controls (maximum cross roll and yaw controls) with an active ARI system. This shortcoming can be effectively resolved by deactivating the departure-prevention devices at the appropriate time and bringing in the spin-prevention system. Thus, ideally, use of both spin- and departure-prevention systems should be considered for fighter aircraft so that the desired combination of high maneuverability and departure/spin resistance is attained.

FUTURE CONCEPTS AND APPLICATIONS

Operational experience with the latest series of fighters has verified that proper control-system design can significantly enhance the departure/spin resistance of fighter aircraft. It is expected, therefore, that this technique will be further developed for application to future configurations. Although it should be possible to use the current high-angle-of-attack control concepts on these advanced designs, it is likely that these advanced vehicles will exhibit aerodynamic characteristics that are significantly different from those of current fighters. Furthermore, future configurations will probably employ unusual types of controls, such as canards and thrust vectoring, and use them in novel ways. All these factors will introduce new high-angle-of-attack problems, the solutions for which will require further development of the control-system design approach. It is beyond the scope of this paper to discuss in any detail all these potential future concepts and problems. Rather, the remainder of the paper is a discussion of one concept, the CCV principle of relaxed static stability (RSS). This principle will very likely be incorporated in future fighters, but it has serious implications on the high-angle-of-attack control problem.

RSS involves designing the airframe so that it has low or negative inherent static longitudinal stability and using the control system to artificially provide the required level of stability; the F-16 airplane employs this design concept. The potential performance benefits of this concept are well known and fighter designs which incorporate very high levels of inherent longitudinal instability are now being considered. The use of RSS, however, can also introduce potential stability and control problems at high angles of attack in addition to the more familiar lateral-directional problems discussed previously.

The fundamental aerodynamic characteristics of RSS configurations which can result in these problems are illustrated in figure 26, which shows an idealized plot of aerodynamic pitching-moment coefficient C_m versus angle of attack which might be expected for a statically unstable configuration. The two main potential problem areas are indicated by the hatched regions as an indication of where they are likely to occur. The lower angle-of-attack region below maximum lift represents an area of susceptibility to uncontrollable pitch departures due to lack of sufficient aerodynamic nose-down control moment. As indicated, if the angle of attack exceeds α_{crit}, additional nose-down moment cannot be generated and the airplane pitches up into an out-of-control situation. Thus, a critical requirement of the control system in this case is to limit the maximum angle of attack to values where control can be maintained. Note, however, that in the angle-of-attack region immediately below α_{crit} there is very little nose-down moment available to prevent angle-of-attack excursions above α_{crit}. For angles of attack higher than α_{crit}, it is seen that the C_m curves change slope because of increasing breakdown of the flow over the entire configuration. This causes the aerodynamic center to move aft, which results in stable deep-stall trim points at very high angles of attack. If the airplane enters these deep-stall trim points, recovery may be very difficult since aerodynamic controls are generally not very effective at these extreme angles of attack.

In summary, RSS configurations can be susceptible to pitch departures at high angles of attack when there is insufficient nose-down aerodynamic moment to prevent angle of attack from increasing above some critical limit beyond which the airplane cannot be controlled in pitch. Two dynamic phenomena which can generate large-angle-of-attack excursions during high-angle-of-attack maneuvering are kinematic coupling and inertia coupling. As discussed in a previous section, substantial increases in angle of attack can be generated kinematically by rolling with proverse sideslip; in addition, large angle-of-attack excursions can occur during recoveries from steep attitude climbs to very low airspeed. Inertially, significant nose-up moments are generated during stability-axis rolling at high angles of attack. If these moments are greater than the available nose-down aerodynamic moment, a pitch departure is likely to occur. This problem is further illustrated in figure 27.

The variation with roll rate of the nose-up inertia coupling moment caused by stability-axis rolling is shown in figure 27. As noted previously, the moment varies with p_s^2 so that very substantial moments can be produced at high roll rates. Also shown are representations of the available nose-down control moment for a specified angle of attack at two values of dynamic pressure, $\bar{q}_1$ and $\bar{q}_2$ $\left(\bar{q}_1 < \bar{q}_2\right)$. The points of intersection with the coupling-moment curve indicate the highest roll rates $\left(p^*_{s,1}\right.$ and $\left.p^*_{s,2}\right)$ at which sufficient control moment exists to counter the nose-up coupling moment. If the roll rate should increase and be sustained above these values, then it is

very likely that a pitch departure will occur. Note that $p^*_{s,1} < p^*_{s,2}$, which indicates that the susceptibility to this type of departure becomes more acute as airspeed decreases. Once a departure beyond the critical angle-of-attack limit occurs, the airplane is likely to continue to pitch up to very high angles of attack and potentially restabilize in a deep-stall trim point as indicated in figure 26. Furthermore, the results of figure 27 point out a rather unique characteristic of RSS configurations – that the maximum sustainable roll rates that can be controlled at high angles of attack may be limited by the effectiveness of the nose-down pitch control.

A fighter configuration which exhibits the characteristics discussed in this section was recently studied in wind-tunnel and piloted simulation investigations at Langley Research Center. (See ref. 8.) The airplane was designed to operate at very moderate inherent levels of pitch instability (Static margin ≈ -0.04) and incorporated a conventional aft-mounted all-moveable horizontal stabilator for pitch control. The configuration had a moderately swept wing and a highly swept wing-body strake to enhance lift and maneuverability at high angles of attack.

Variations with angle of attack of the pitching-moment coefficient for neutral, full nose-up, and full nose-down stabilator deflections are shown in figure 28. The data show that the airplane would trim at $\alpha = 66^\circ$ with full nose-up stabilator deflection. To inhibit inadvertent excursions to these extreme angles of attack, the pitch-control system incorporated an angle-of-attack limiter which drove the stabilator in an attempt to keep angle of attack from exceeding 25°. Figure 28 shows, however, a sharp loss in nose-down stabilator effectiveness for $\alpha > 25^\circ$. It was not surprising, therefore, that the airplane exhibited susceptibility to pitch departure caused by the inertia coupling phenomenon discussed previously. Figure 29 shows an example of such a loss-of-control situation encountered during the simulation study of this configuration. An attempted 360° roll is shown with full lateral-stick input applied at $\alpha = 25^\circ$ in an accelerated turn. In addition to maximum roll-control deflections, maximum coordinating rudder was also obtained to make the airplane roll about the velocity vector. As a result, the body-axis roll and yaw rates began to build up rapidly in the direction of the stick input. Initially, α dropped slightly because of kinematic coupling; however, as p and r increased, the inertia coupling moment caused a significant nose-up pitch rate to build up, and α began to increase. At this point, q coupled with p to create a yaw coupling moment which opposed the yaw rate and halted its growth ($t \approx 14$ sec); on the other hand, p was still increasing and thus resulted in the kinematic generation of a large amount of adverse sideslip ($t \approx 15$ sec). By this time, α had increased to above 30° despite the angle-of-attack limiter system applying full nose-down stabilator deflection (25°). The nose-up inertia coupling moment was much greater than the nose-down aerodynamic moment produced by $\delta_h = 25^\circ$; as a result, a pitch departure occurred as the airplane completed

about 270^{o} of the roll, just after $t = 15$ sec. During the ensuing loss-of-control period, α reached a maximum of 68^{o} while β oscillated between 26^{o} and -26^{o}.

The foregoing results showed that the airplane roll-rate capability at high angles of attack was too high to prevent pitch departures with the available pitch control, and that the only means of alleviating the pitch departure problem (other than resizing the control surfaces or further constraining maximum angle of attack) was to properly design the control system to reflect this fact. The control-system features developed to achieve this goal are summarized conceptually in figure 30. Obviously, an essential element is a roll-rate limiter system which inhibits the roll rate from exceeding the critical values which result in inertia coupling departures. Four parameters were used to evaluate what the roll-rate limit should be at any given time – dynamic pressure, angle of attack, symmetric stabilator deflection, and roll-rate magnitude. Angle of attack was chosen for two reasons: (1) the nose-up inertia-coupling moment varies with $\sin 2\alpha$; and (2) the amount of nose-down control moment available to counter the nose-up coupling moment decreases as angle of attack increases. Similar reasoning was used in choosing $\bar{q}$. Symmetric stabilator deflection was chosen because it directly indicates the pitch control remaining to oppose the inertia-coupling moment. Finally, roll-rate magnitude was used to schedule the total level of limiting imposed. For low roll rates, where coupling is not a factor, no limiting was imposed regardless of the values of the other scheduling parameters. The limiting schedule was used only when the roll rate approached significant magnitudes. With this scheme, the initial roll-response degradation was minimized and roll performance was compromised only where it was essential to prevent occurrence of the pitch departure.

A second feature was incorporated to minimize the generation of proverse sideslip during rolls at high angles of attack. As discussed previously, rolling with proverse sideslip increases angle of attack through kinematic coupling and is therefore not desirable for RSS configurations for which there is a requirement to maintain angle of attack below some critical value. Proverse sideslip minimization was accomplished by scheduling the maximum rudder deflection that the pilot could command through his pedals as a function of angle-of-attack and roll-rate magnitude such that at significant values of α and $|p|$, no deflection could be commanded. In this situation, the only direct rudder response to pilot inputs came from coordinating rudder deflections commanded by the roll-control input. Hence, no overcoordination of high-angle-of-attack rolls was possible.

The final feature incorporated in the control system to inhibit the pitch departure was an inertia-coupling compensator for the pitch axis to assure proper stabilator response during high-angle-of-attack rolling maneuvers. The system used angle-of-attack and roll-rate magnitude to drive the pitch control in the nose-down direction to oppose the nose-up coupling moment.

The effectiveness of the preceding control-system design in preventing inertia-coupling departures is illustrated in figure 31, which shows a 360° roll using full lateral stick applied at $\alpha = 25^{\circ}$ in an accelerated turn. As discussed previously, this maneuver performed with the basic airplane resulted in loss of control. (See fig. 29.) However, the maneuver could be completed with the modified control system. Although the pilot applied and held full roll command, the system began to decrease the roll-control deflection as the roll rate approached critical values above which there would not be sufficient nose-down control to oppose the coupling moment. Note that near the completion of the maneuver, only about 25 percent of maximum roll-control surface deflection (authority of $\pm 20^{\circ}$) was used. Because roll rate was properly limited, the stabilator never reached its maximum deflection, and consequently no departure occurred. Angle of attack did not exceed the 25° limit and the maximum sideslip generated was only 3°.

As discussed previously, the second major high-angle-of-attack control problem introduced by use of the RSS concept is the potential for deep-stall trim. As shown in figure 28, the subject configuration exhibited a weak but stable deep-stall trim at $\alpha \approx 60^{\circ}$ even with full nose-down stabilator deflection. Two techniques were found for generating a pitch departure which would result in angle-of-attack excursions into the deep-stall region. The first technique was the coupling departure discussed in the preceding section of this paper. This departure, however, could essentially be eliminated by the control-system design discussed previously. However, a second deep-stall entry technique was found which the control system was unable to prevent. The maneuver involved putting the airplane into a steep, nose-up-attitude, decelerating climb with θ reaching a maximum of about 70° and allowing airspeed to bleed off to about 35 KIAS at the top of the climb. The airplane was then allowed to fall through at essentially zero g. The resulting kinematic generation of a large angle-of-attack excursion could not be effectively opposed by the pitch control because of the very low level of dynamic pressure involved. Once the airplane was stabilized in a deep stall, no recovery was possible because the angle-of-attack limiter system commanded full nose-down control deflection independent of pilot input. To correct this deficiency, the control system was modified such that it was possible to reconfigure the pitch-control law in the event of a deep-stall entry. The reconfiguration involved deactivating all feedback, including the angle-of-attack limiter system so that the only signal that remained was the pilot stick command. With this system, the pitch control deflected directly proportional to pilot inputs. The reason for doing this can be seen by reviewing the pitching-moment data for the maximum stabilator deflections shown in figure 28. The data show that at the deep-stall trim point ($\alpha \approx 60^{\circ}$), a comparatively large pitching-moment increment results in going from full nose-down to full nose-up control deflection $\left(\Delta C_m \approx 0.1\right)$. Thus, a possibility exists to use this available control moment to initiate and build up a pitch oscillation by moving the stick in phase with the airplane motions. This would be done with the hope that

sufficient angular momentum would be created during a downswing cycle to drive the airplane over the positive C_m "hump" and back down to within the normal angle-of-attack envelope of the airplane.

A recovery attempt using the pitch oscillation technique is shown in figure 32. The nose-high decelerating-climb technique was used to cause the airplane to enter the deep-stall trim point. Starting from this stabilized trim at $\alpha \approx 62^{\circ}$, the pilot reconfigured the control system and rapidly applied full aft stick at $t = 71.3$ sec. The resulting nose-up moment caused α to increase to 75°, at which point the pilot reversed his controls and applied full forward stick. About 14 deg/sec nose-down pitch rate resulted and the associated angular momentum was sufficient to cause the airplane to continue to pitch downward until a recovery was obtained at $t = 78$ sec. Although the rapidity of the recoveries obtained was dependent on proper phasing of pilot inputs, this technique was found to be consistently effective in providing recoveries from the deep-stall trim exhibited by this configuration.

To summarize this discussion of the impact of RSS, the foregoing results have shown how proper control-system design can significantly alleviate the high-angle-of-attack problems of pitch departure and deep stall that can result from applying the RSS concept to fighter aircraft. Control-system concepts that enhance resistance to pitch departure are angle-of-attack limiting and roll-rate limiting. Because of the ability of RSS configurations to trim to extreme angles of attack, some form of angle-of-attack limiting system is normally required and selecting the limit angle of attack to be as low as possible maximizes the resistance to pitch departure. Naturally, the effectiveness of this approach is constrained by performance considerations which are a critical factor in determining the angle-of-attack limit value to be used. Once an angle-of-attack limit is selected, further enhancement of resistance to pitch departure can be attained by designing the control system such that a proper balance is achieved between roll performance capability and available nose-down aerodynamic control moment. This may involve some form of roll-rate limiting and other features to inhibit the generation of proverse sideslip during rolls at high angles of attack. With regard to the deep-stall problem, recovery potential can be enhanced by incorporating the capability to reconfigure the pitch-control system such that the nominal feedback paths, and in particular the angle-of-attack limiter, are deactivated so that the pilot has direct control of the pitch control with which to attempt to oscillate the airplane out of the trim point. For new airplanes, of course, it would be more desirable to design the airframe so as to preclude the existence of a stable deep-stall trim condition. (See ref. 9.)

CONCLUDING REMARKS

The present paper is a summary of the experience gained at the NASA Langley Research Center in the area of control-system techniques for enhancing the departure/spin resistance of fighter aircraft. The reader should be aware that this paper does not constitute a complete and exhaustive study, since high-angle-of-attack aerodynamics are known to be quite configuration-dependent. Rather, this study was focused on key aerodynamic stability and control characteristics that are common to most current fighter configurations and are important to control-system design. Experience at Langley to date has shown that proper control-system design can be an effective approach for attaining the goal of high maneuverability combined with good resistance to departures and spins. Operational experience with the latest fighter designs has confirmed these results. In view of these successes, further development of this approach is required to maximize the benefits that can be realized in applications to future fighter aircraft.

From the analysis presented in this paper, several important conclusions are summarized as follows:

1. The strong dependence of key aerodynamic stability and control derivatives, including both static and damping derivatives, upon angle of attack and Mach number should be carefully considered in control-system design for high-angle-of-attack flight conditions.

2. Control systems designed without proper consideration for the high-angle-of-attack aerodynamics and flight mechanics phenomena noted in this study can often have detrimental effects on airplane departure/spin resistance.

3. Several of the pilot control techniques that have been applied effectively to airplanes having conventional stability augmentation systems can cause unexpected stall entries and degraded high-angle-of-attack handling qualities if applied to airplanes using high-authority command augmentation systems (CAS). Therefore, considerable care should be taken in training pilots for transition from old to new airplanes to insure that the unique control characteristics of CAS airplanes are well understood.

4. Properly designed aileron-rudder interconnect systems and stability-axis yaw dampers can provide improved departure/spin resistance, improved Dutch roll damping, and improved roll performance at high angles of attack.

5. In the design of roll dampers used at high angles of attack, careful attention must be paid to the airplane lateral-directional static stability and control characteristics to insure that favorable rather than adverse effects are obtained; proper system limiting must be observed to avoid degrading departure/spin resistance at high angles of attack.

6. Proper high-angle-of-attack control-system design should consider the use of all available control moments for stability augmentation and control, including those that are conventionally considered adverse since these control moments can often be quite powerful in the stall region.

7. Use of both departure- and spin-prevention systems should be considered for fighter aircraft to obtain the desired combination of high maneuverability and high departure/spin resistance.

8. For fighter configurations incorporating relaxed static stability (RSS), the high-angle-of-attack control-system design must account for both the classic lateral-directional stability and control problems as well as the additional potential problems of pitch departures due to high roll-rate maneuvers and low airspeed maneuvers.

Langley Research Center
National Aeronautics and Space Administration
Hampton, VA 23665
June 5, 1980

REFERENCES

1. Chambers, Joseph R.; and Grafton, Sue B.: Aerodynamic Characteristics of Airplanes at High Angles of Attack. NASA TM-74097, 1977.

2. Ross, A. Jean: Lateral Stability at High Angles of Attack, Particularly Wing Rock. Stability and Control, AGARD-CP-260, May 1979, pp. 10-1 – 10-19.

3. Gilbert, William P.; Nguyen, Luat T.; and Van Gunst, Roger W.: Simulator Study of Applications of Automatic Departure- and Spin-Prevention Concepts to a Variable-Sweep Fighter Airplane. NASA TM X-2928, 1973.

4. Nguyen, Luat T.; Gilbert, William P.; and Van Gunst, Roger W.: Simulator Study of the Departure Resistance of a Lightweight Fighter Airplane With Twin Vertical Tails. NASA TM X-3510, 1977.

5. Gilbert, William P.; Nguyen, Luat T.; and Van Gunst, Roger W.: Simulator Study of the Effectiveness of an Automatic Control System Designed To Improve the High-Angle-of-Attack Characteristics of a Fighter Airplane. NASA TN D-8176, 1976.

6. Gilbert, William P.; and Libbey, Charles E.: Investigation of an Automatic Spin-Prevention System for Fighter Airplanes. NASA TN D-6670, 1972.

7. Chambers, Joseph R.; Bowman, James S., Jr.; and Malcolm, Gerald N.: Stall/Spin Test Techniques Used by NASA. Stall/Spin Problems of Military Aircraft, AGARD-CP-199, June 1976, pp. 13-1 – 13-12.

8. Nguyen, Luat T.; Ogburn, Marilyn E.; Gilbert, William P.; Kibler, Kemper S.; Brown, Philip W.; and Deal, Perry L.: Simulator Study of the Stall/Post-Stall Characteristics of a Fighter Airplane With Relaxed Longitudinal Static Stability. NASA TP-1538, 1979.

9. Nguyen, Luat T.; Gilbert, William P.; and Grafton, Sue B.: Control Considerations for CCV Fighters at High Angles of Attack. Aerodynamic Characteristics of Controls, AGARD-CP-262, Sept. 1979, pp. 11-1 – 11-10.

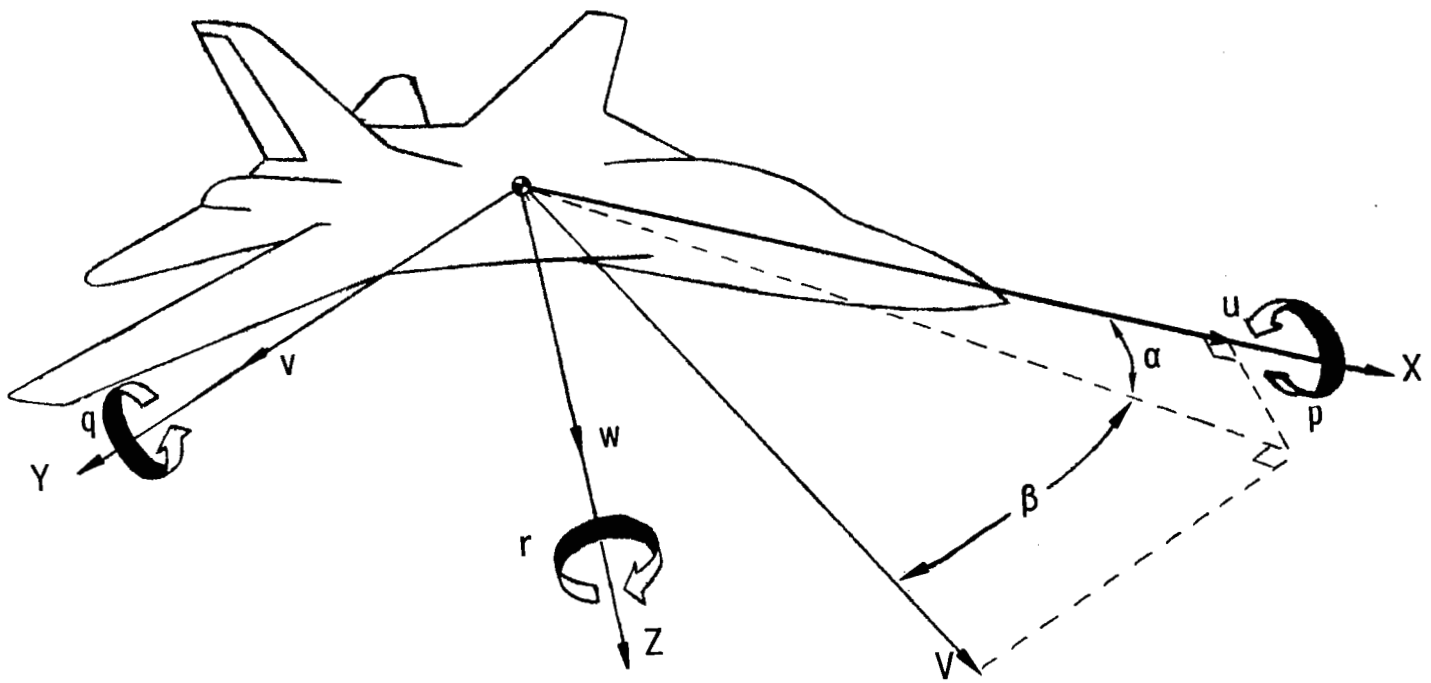

Figure 1.- Body system of axes.

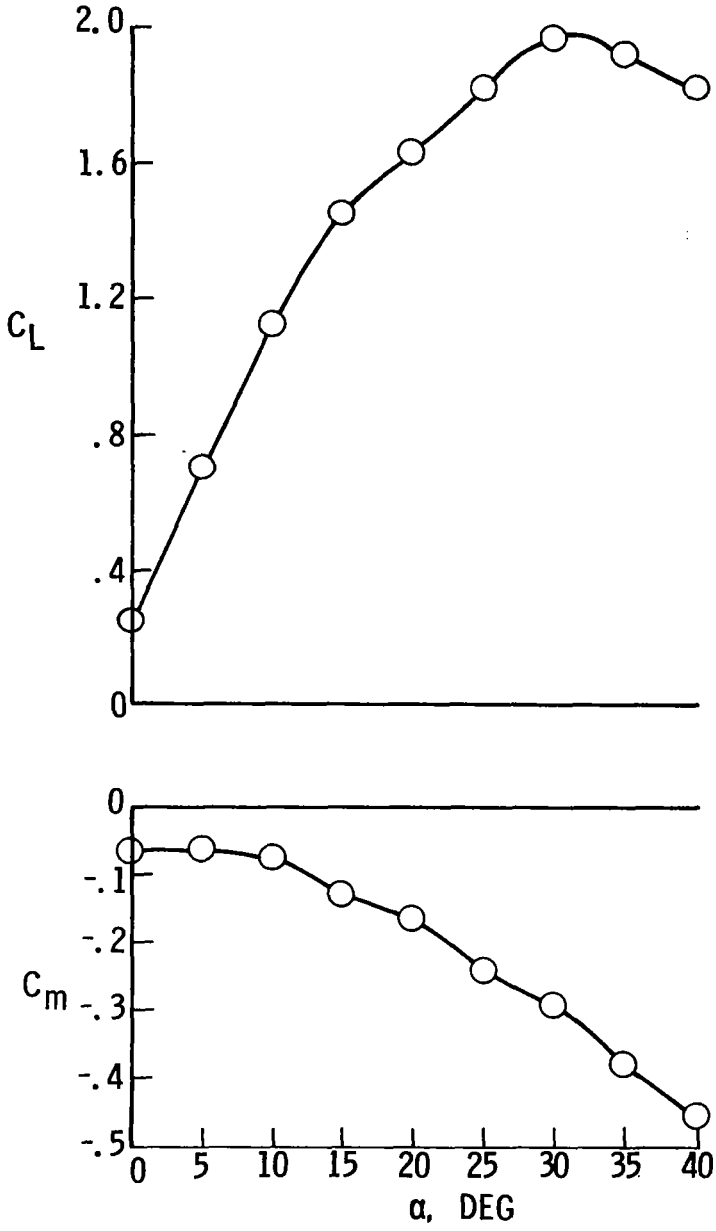

Figure 2.- Variation of low-speed lift and pitching-moment characteristics with angle of attack for a typical modern fighter configuration.

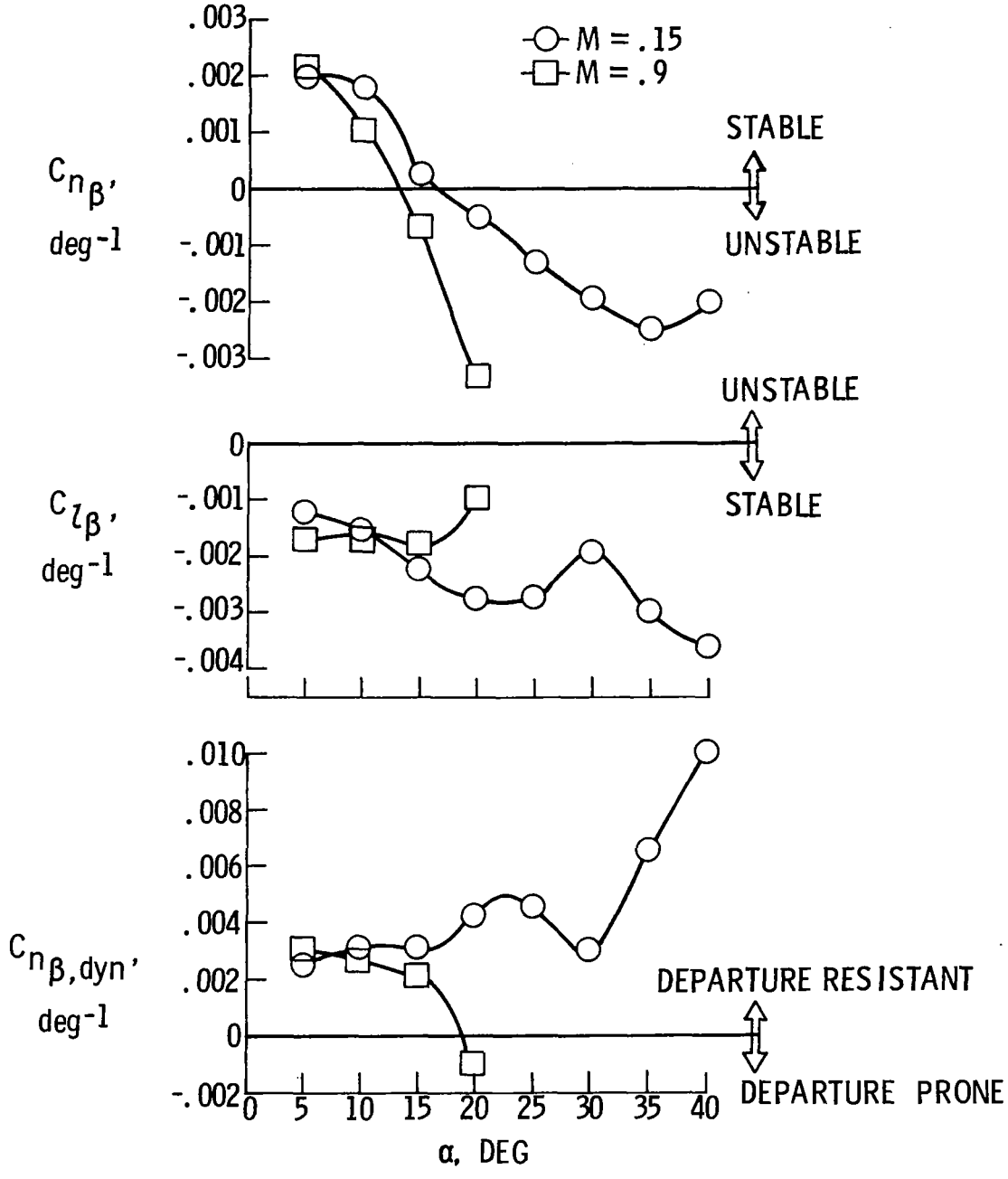

Figure 3.- Variation of static lateral-directional stability characteristics with angle of attack.

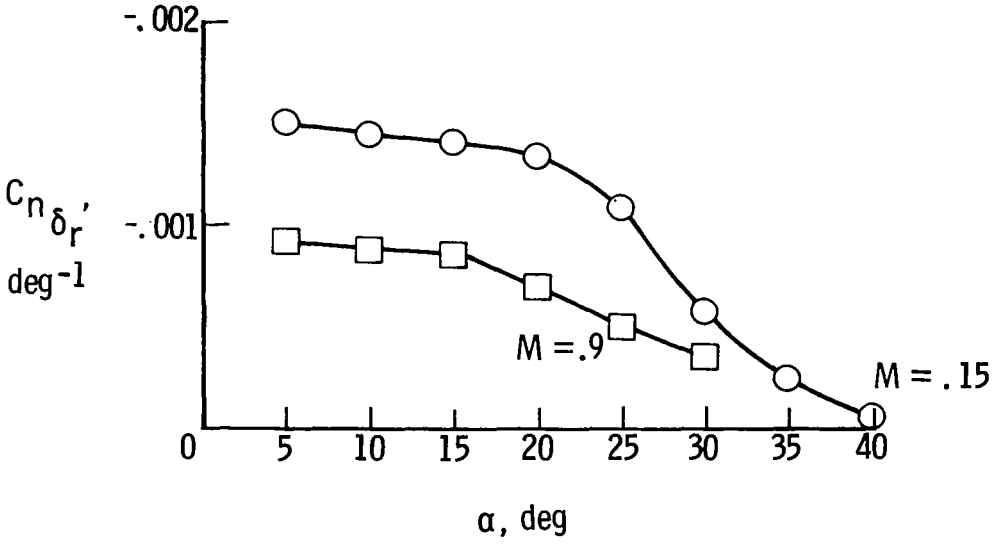

Figure 4.- Variation of rudder yawing-moment derivative with angle of attack.

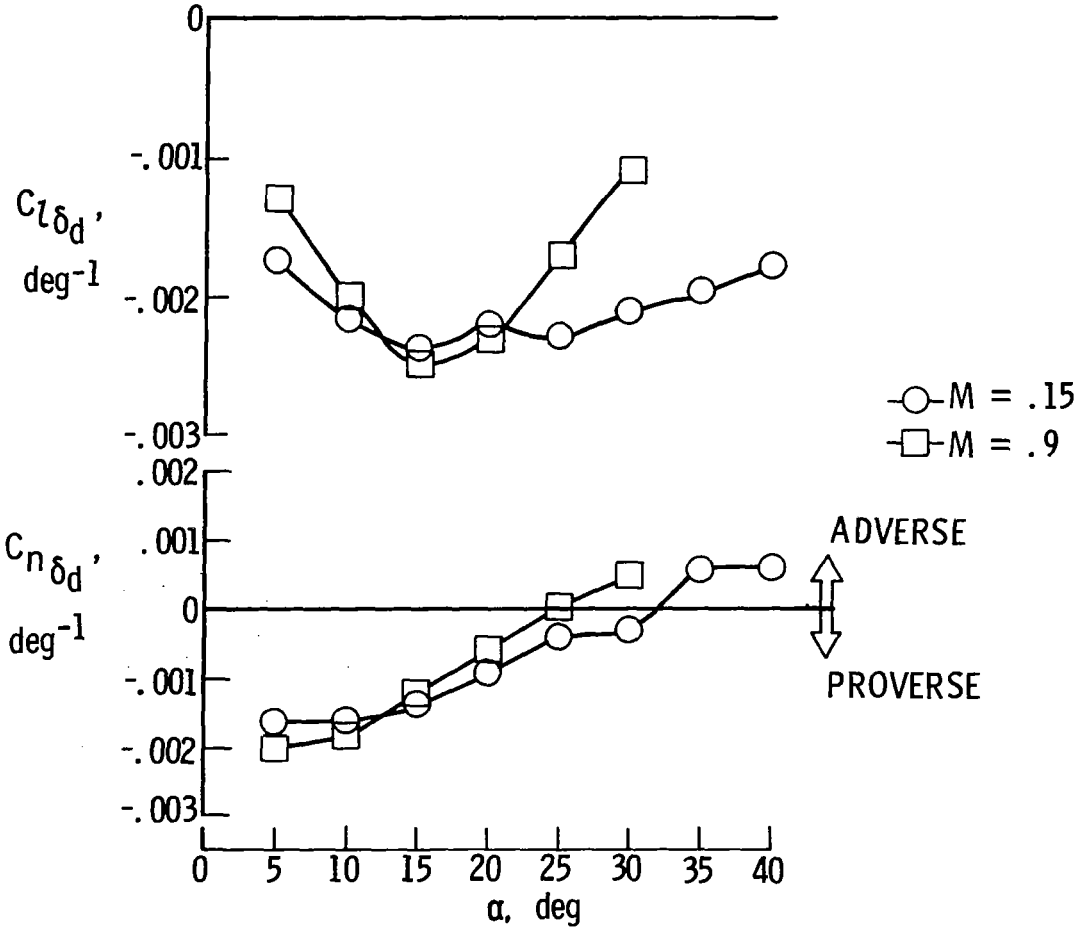

Figure 5.- Variation of differential tail characteristics with angle of attack.

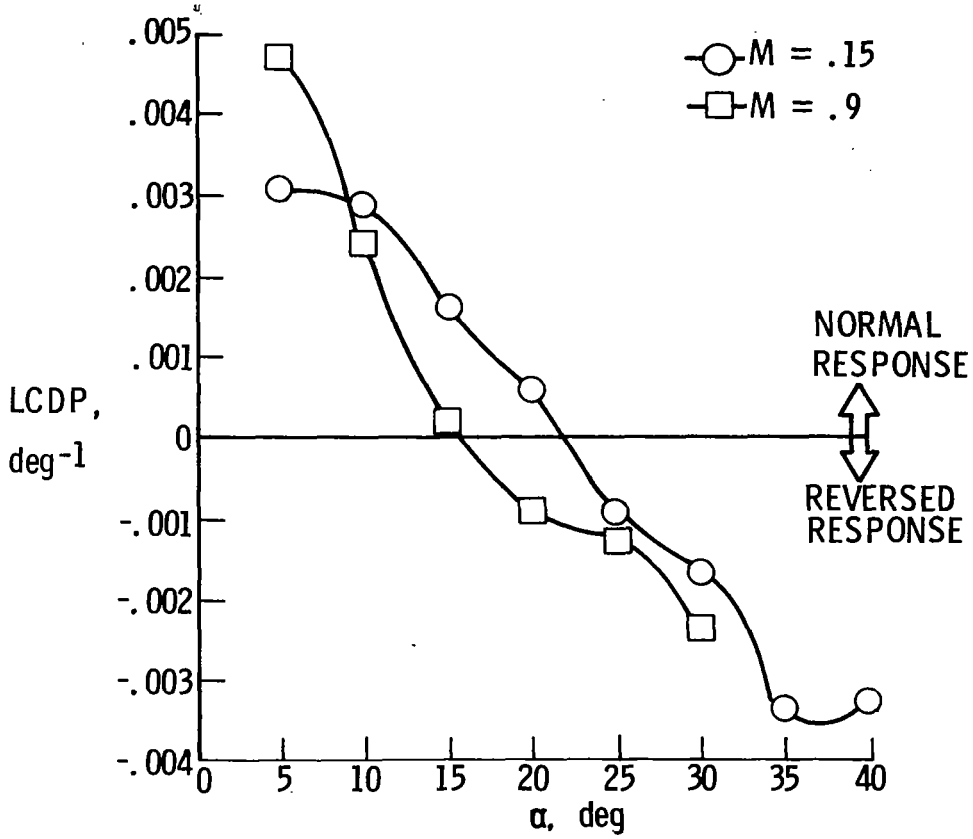

Figure 6.- Variation of lateral control divergence parameter with angle of attack.

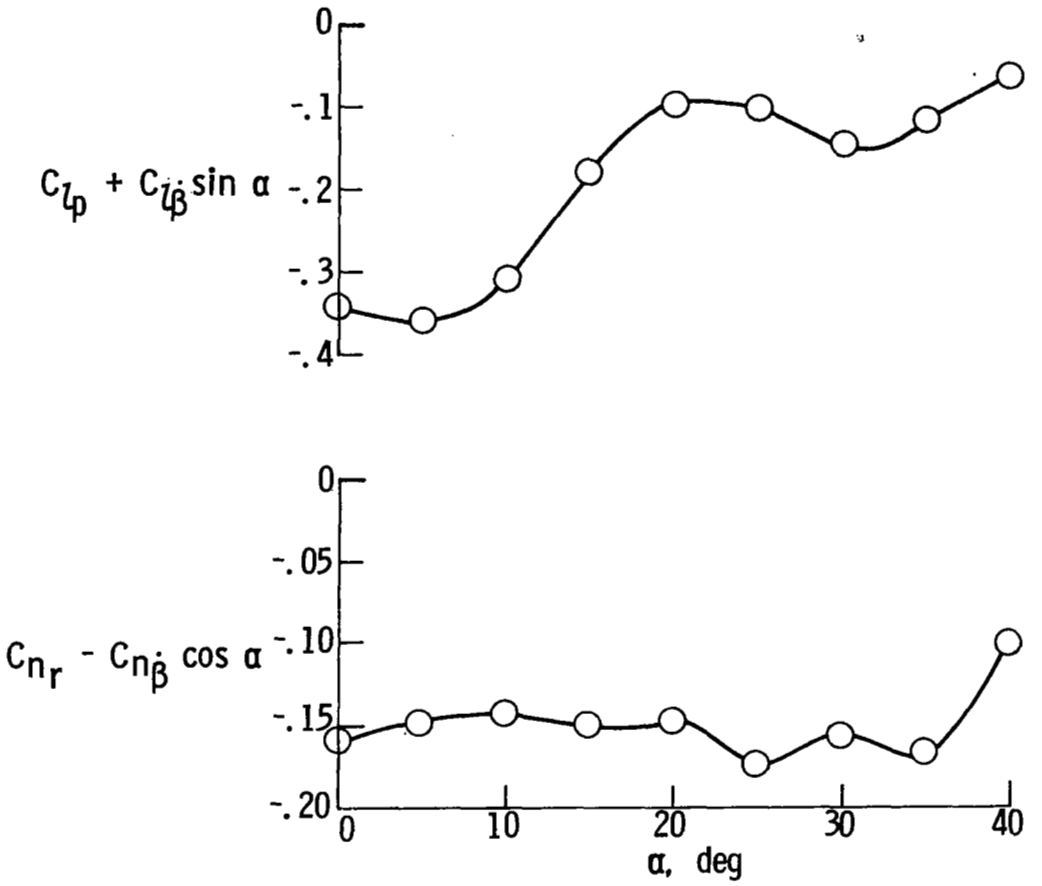

Figure 7.- Variation of low-speed roll and yaw damping derivatives with angle of attack.

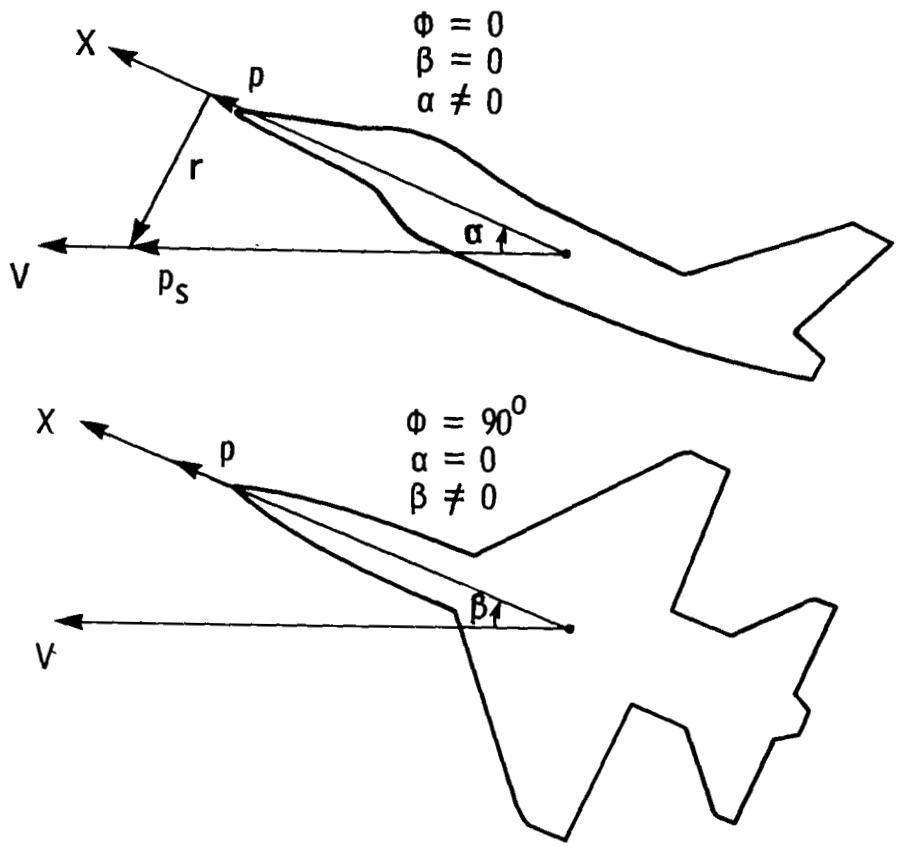

Figure 8.- Illustration of kinematic coupling of angle of attack and sideslip.

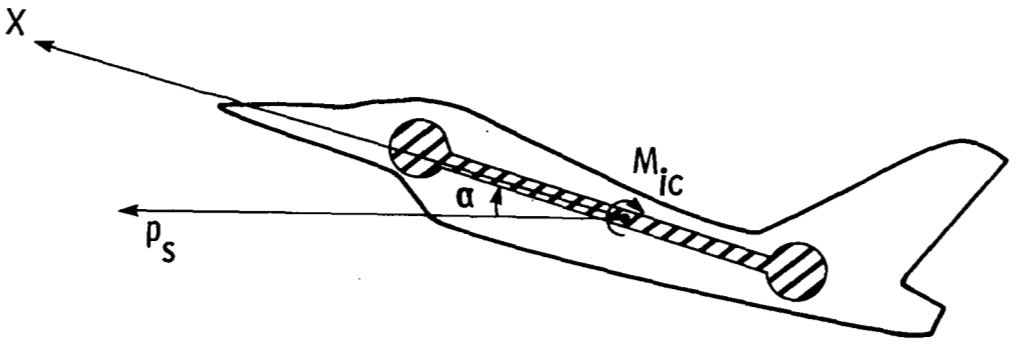

(a) Pitching moment created by roll and yaw rates.

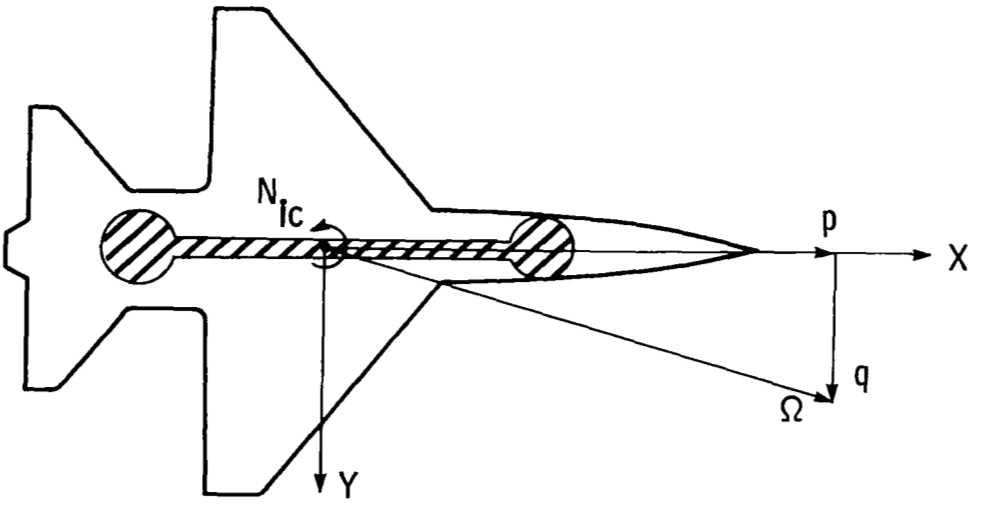

(b) Yawing moment created by roll and pitch rates.

Figure 9.- Illustration of inertia-coupling phenomena.

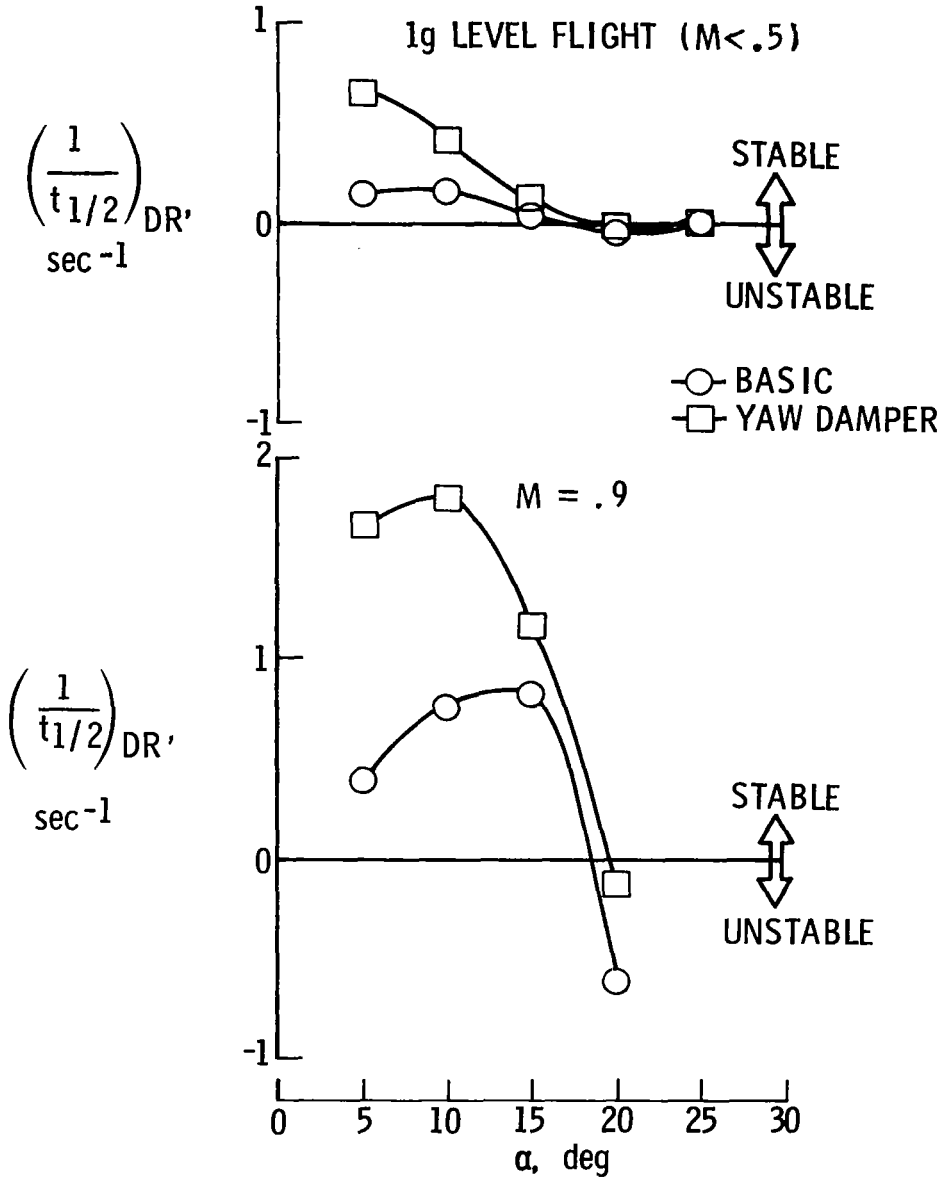

Figure 10.- Example of effects of conventional yaw damper on Dutch roll damping.

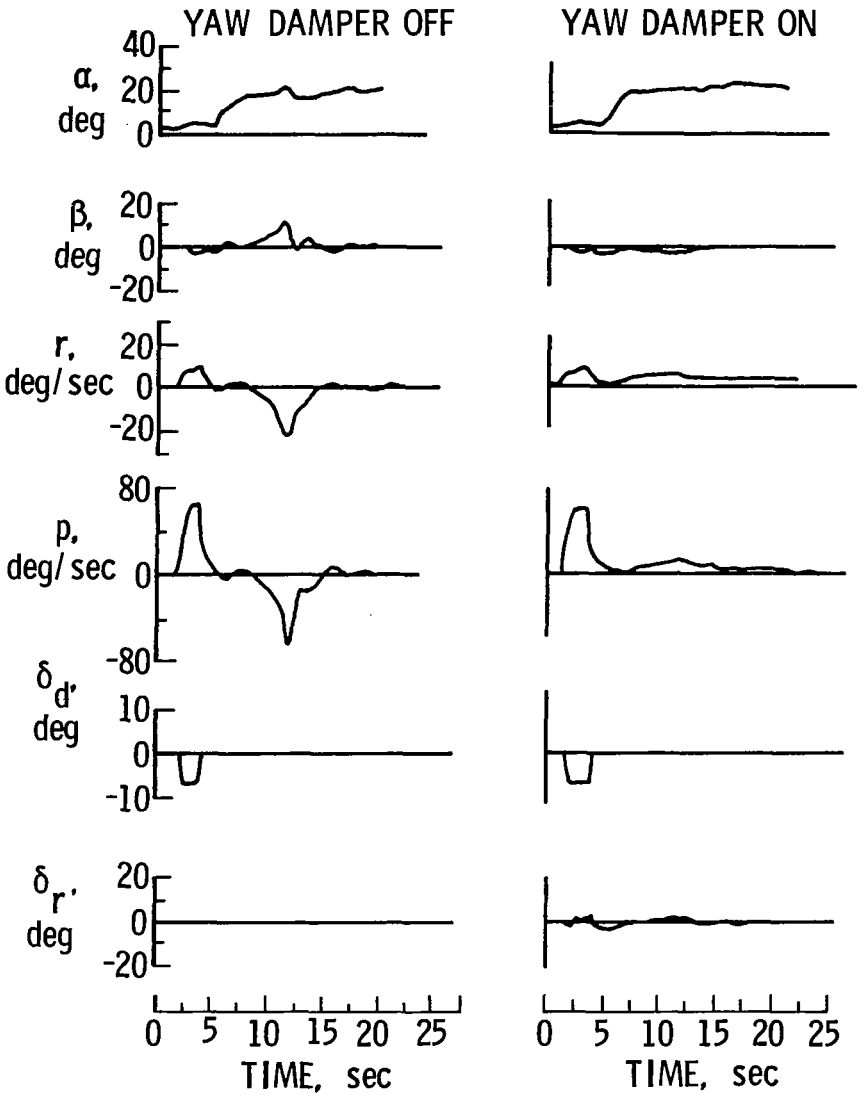

Figure 11.- Time histories of split-S entries into transonic instability region with and without a conventional yaw damper active.

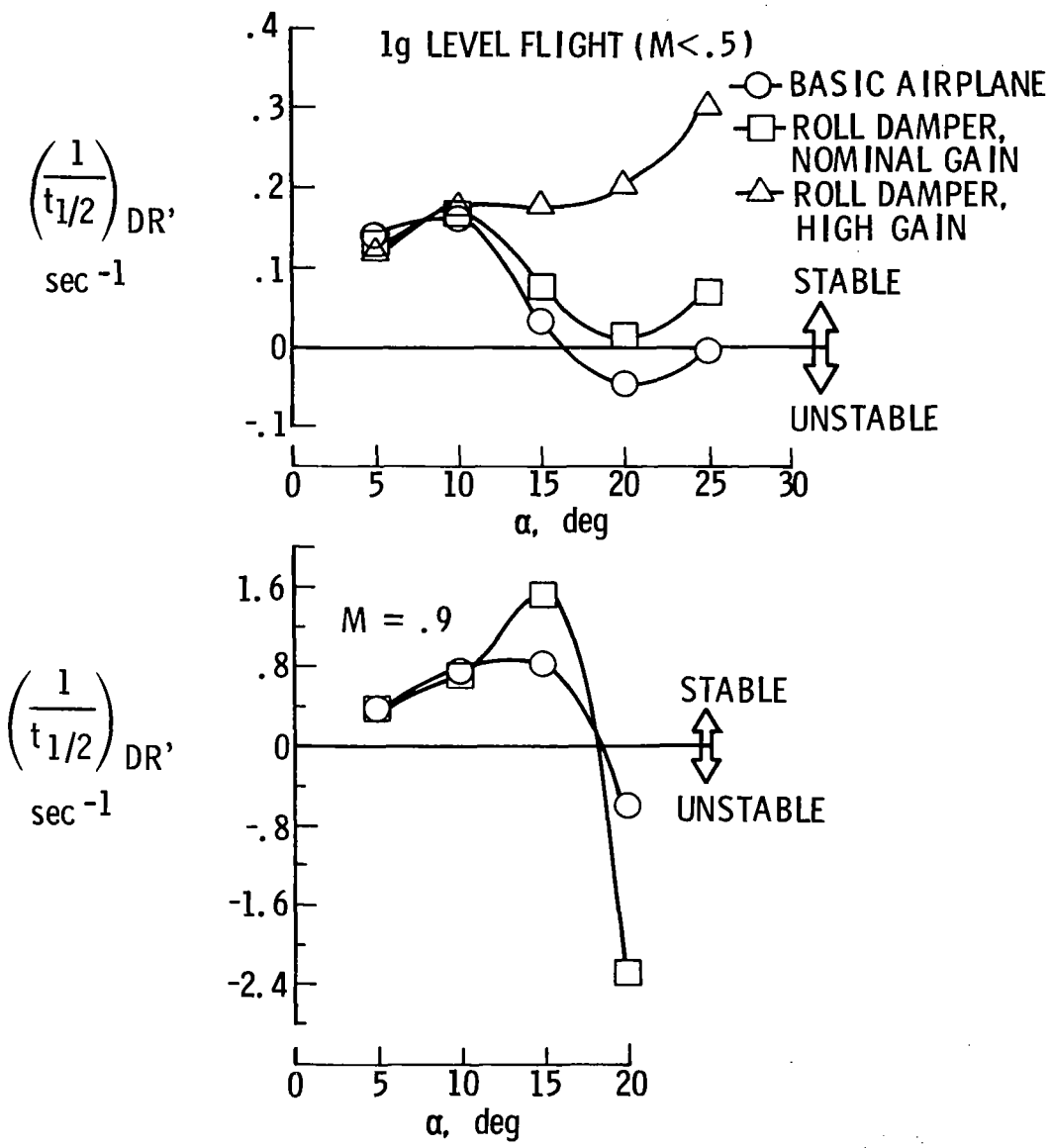

Figure 12.- Example of effect of conventional roll damper on Dutch roll damping.

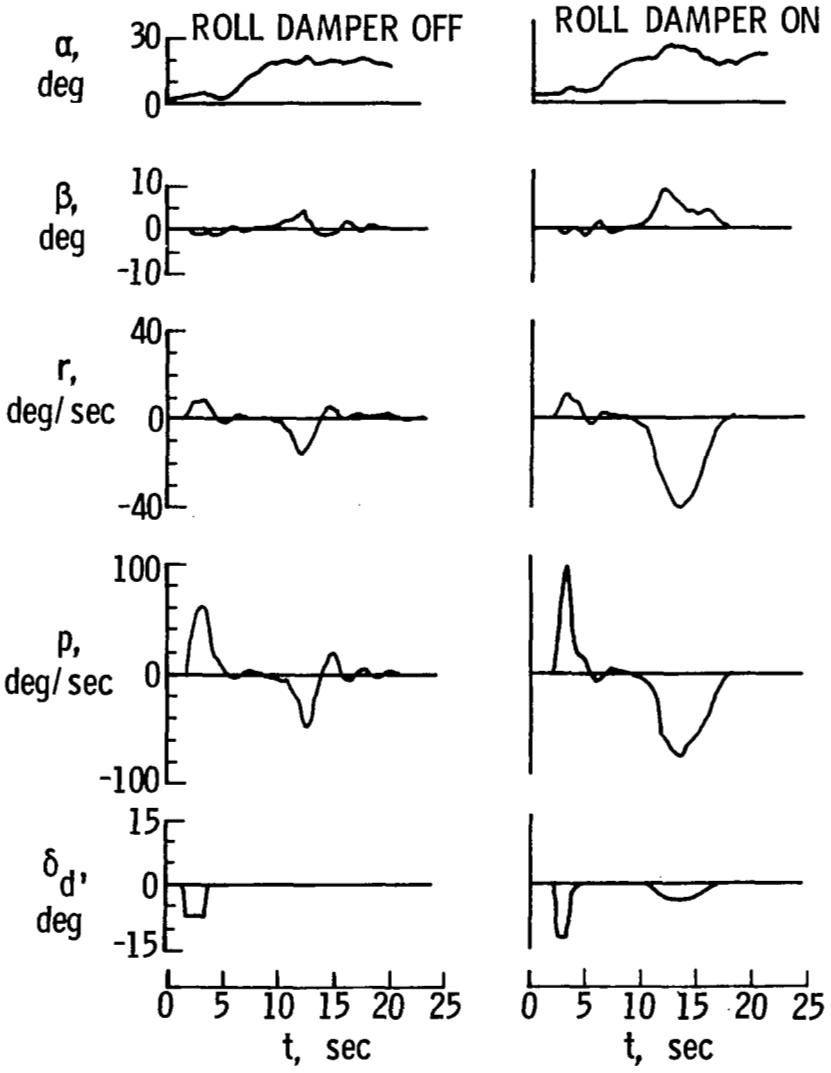

Figure 13.- Time histories of split-S entries into transonic instability region with and without conventional roll damper active.

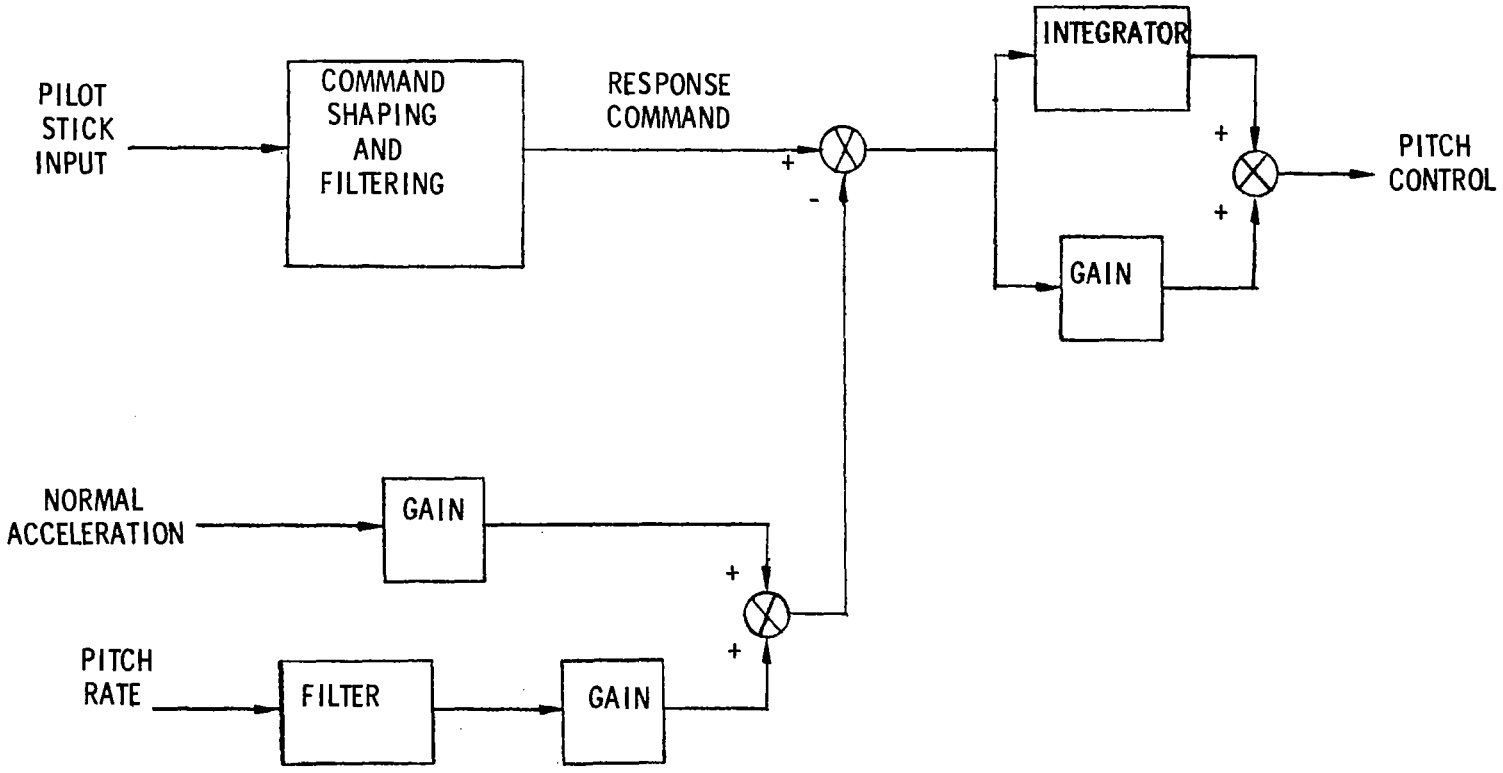

Figure 14.- Typical implementation of pitch command augmentation system.

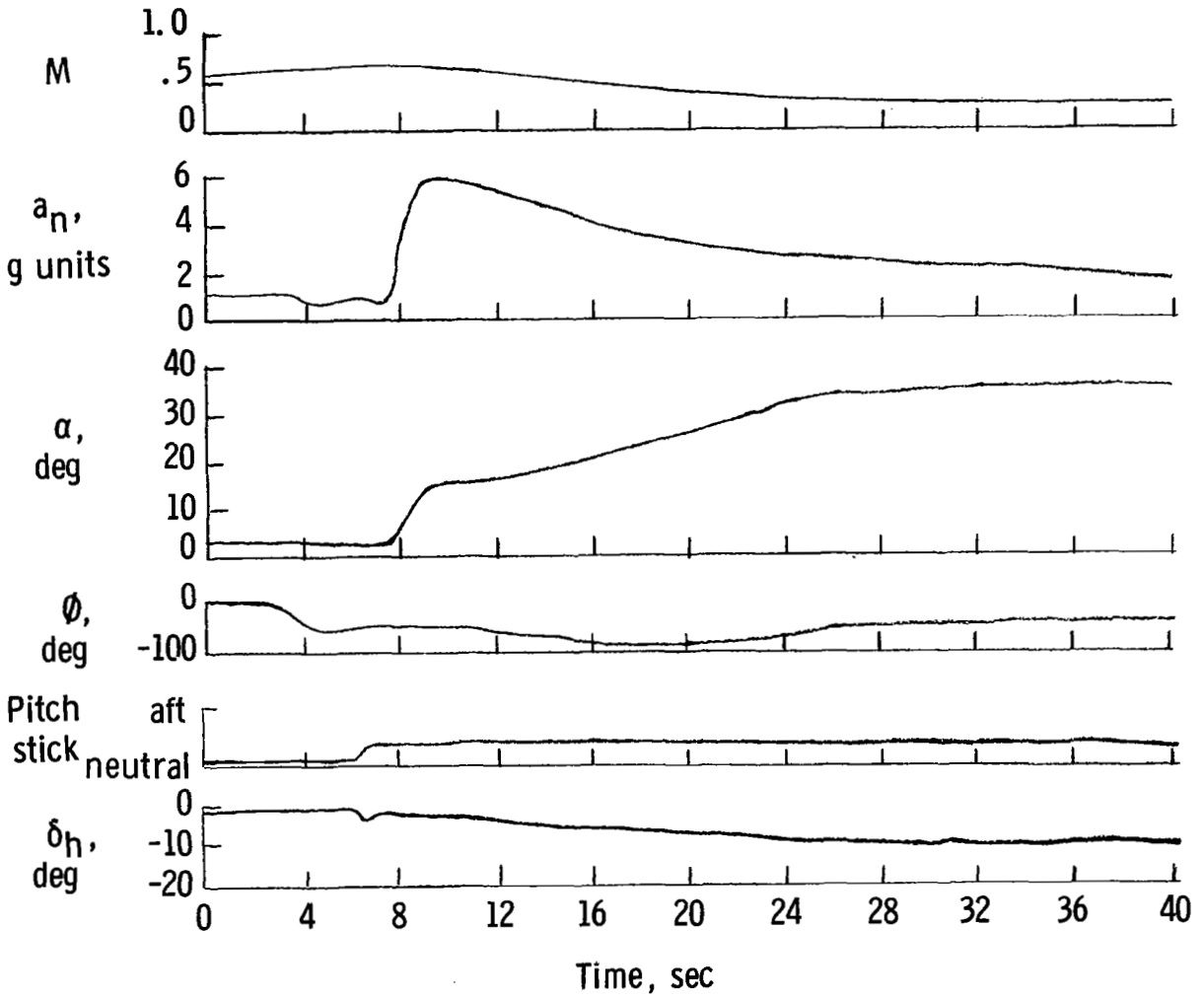

Figure 15.- Example of inadvertent stall entry caused by pitch command augmentation system.

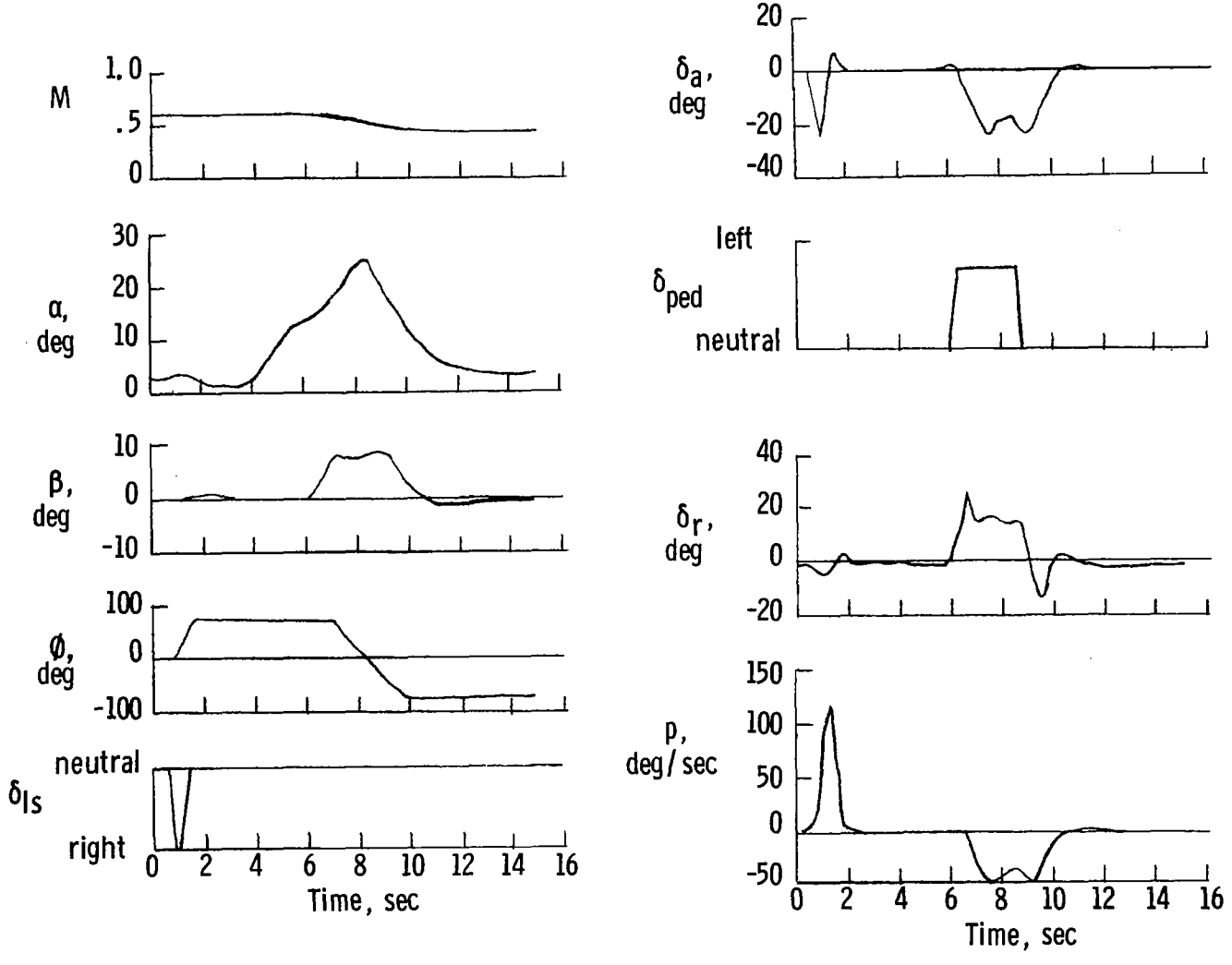

Figure 16.- High-angle-of-attack stick-centered rudder roll on airplane with roll-rate command augmentation system.

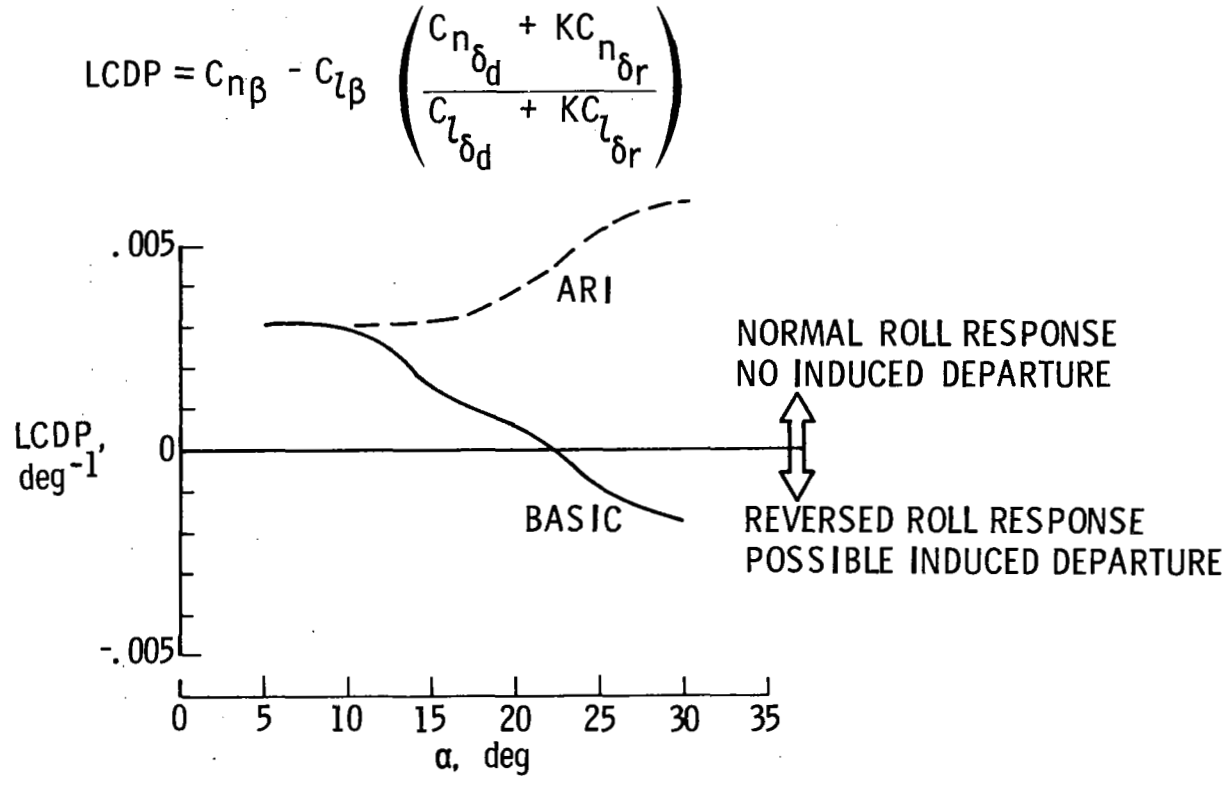

Figure 17.- Example of effect of an ARI system on roll-control effectiveness at high angles of attack.

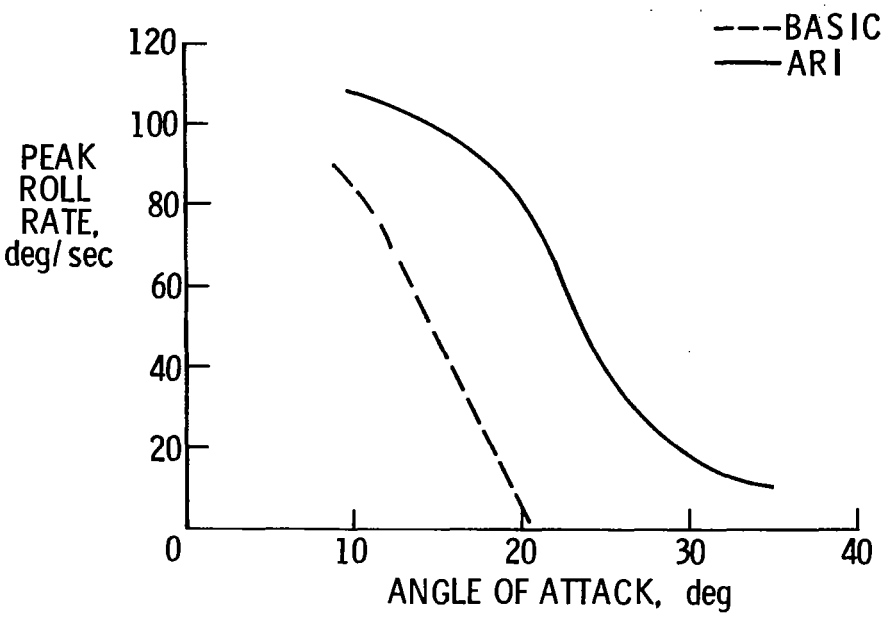

Figure 18.- Example of effect of an ARI system on roll performance.

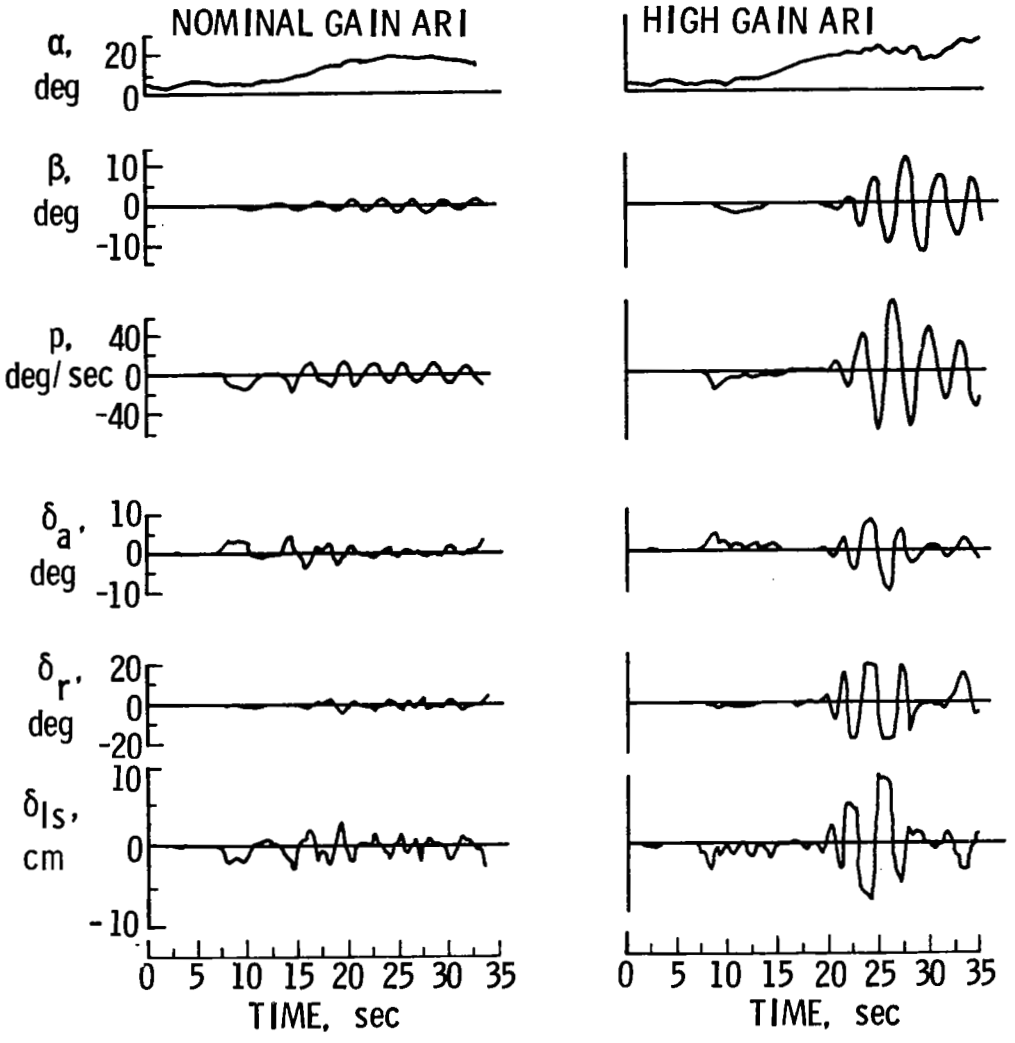

Figure 19.- Tracking time histories illustrating effect of excessive ARI gain on closed-loop stability.

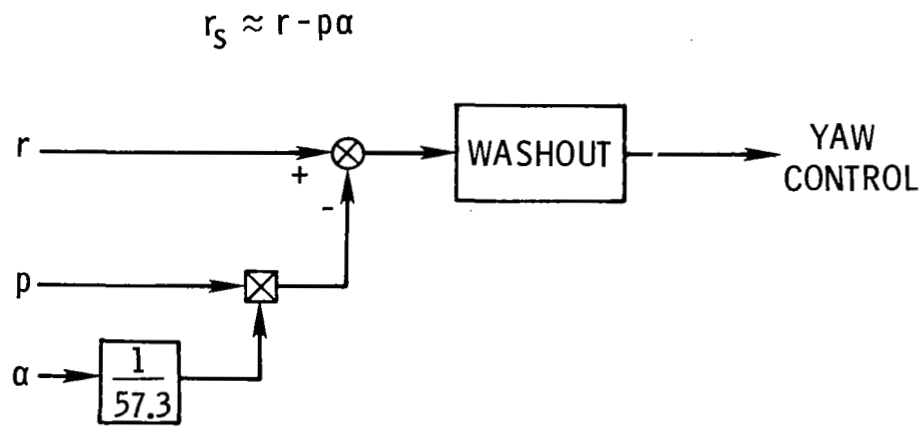

Figure 20.- Typical implementation of stability-axis yaw damper.

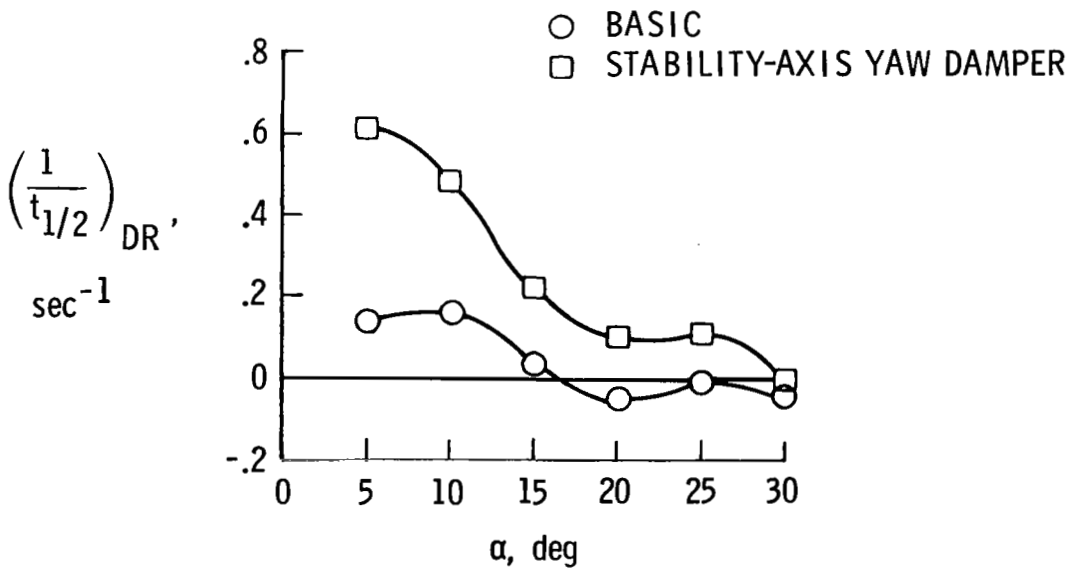

Figure 21.- Example of effect of stability-axis yaw damper on Dutch roll damping.

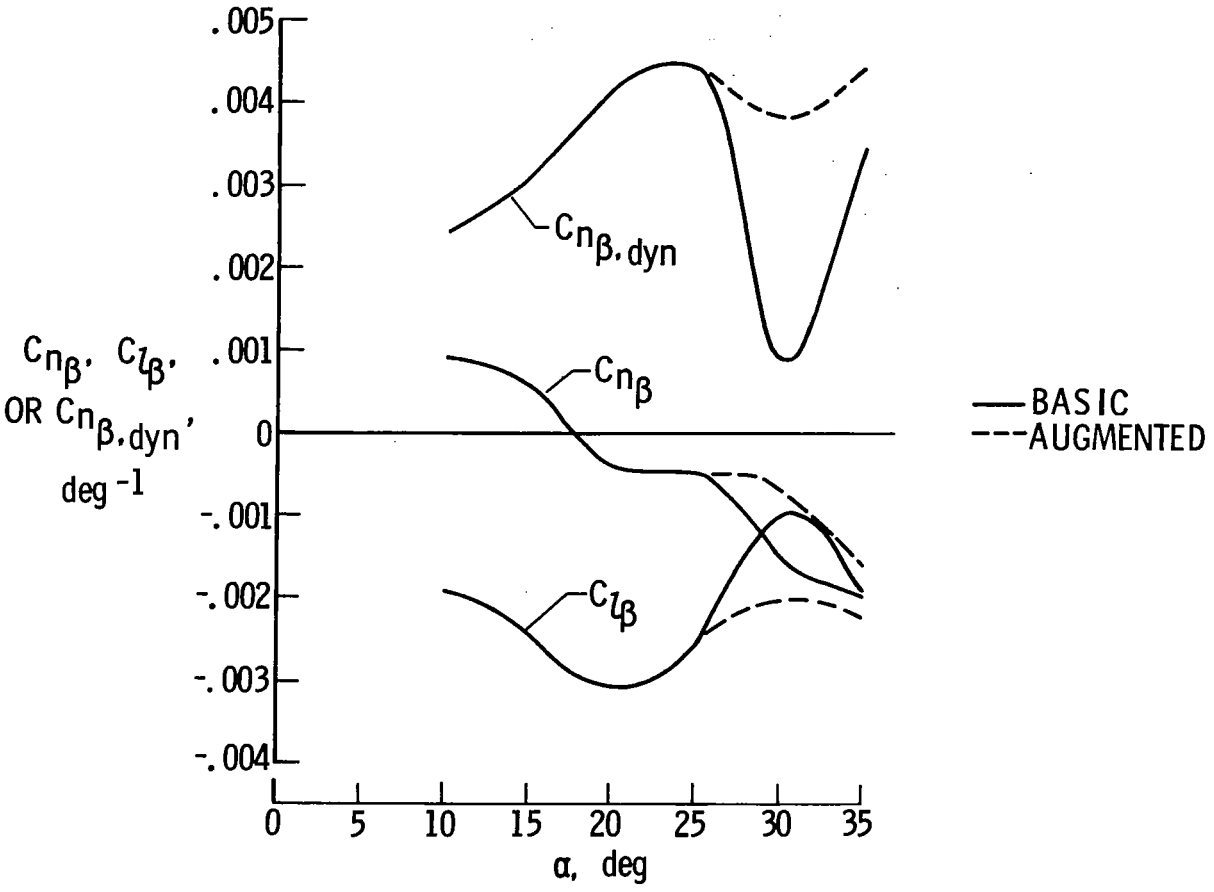

Figure 22.- Example of effectiveness of high-angle-of-attack static stability augmentation.

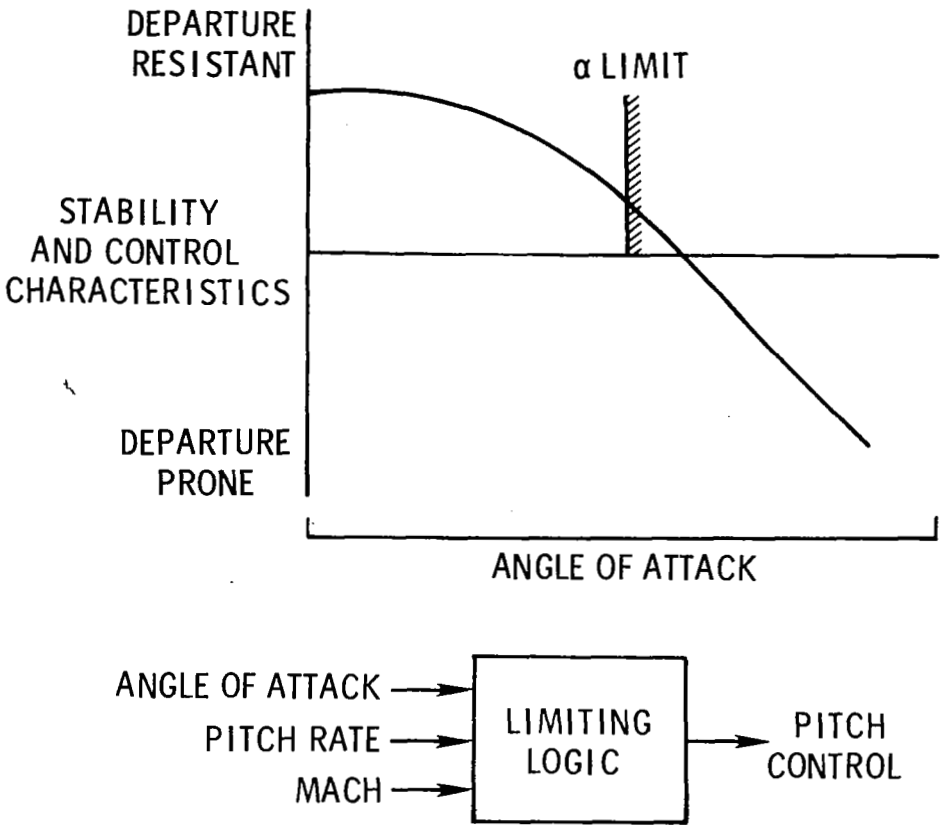

Figure 23.- Conceptual rationale for use of angle-of-attack limiting systems.

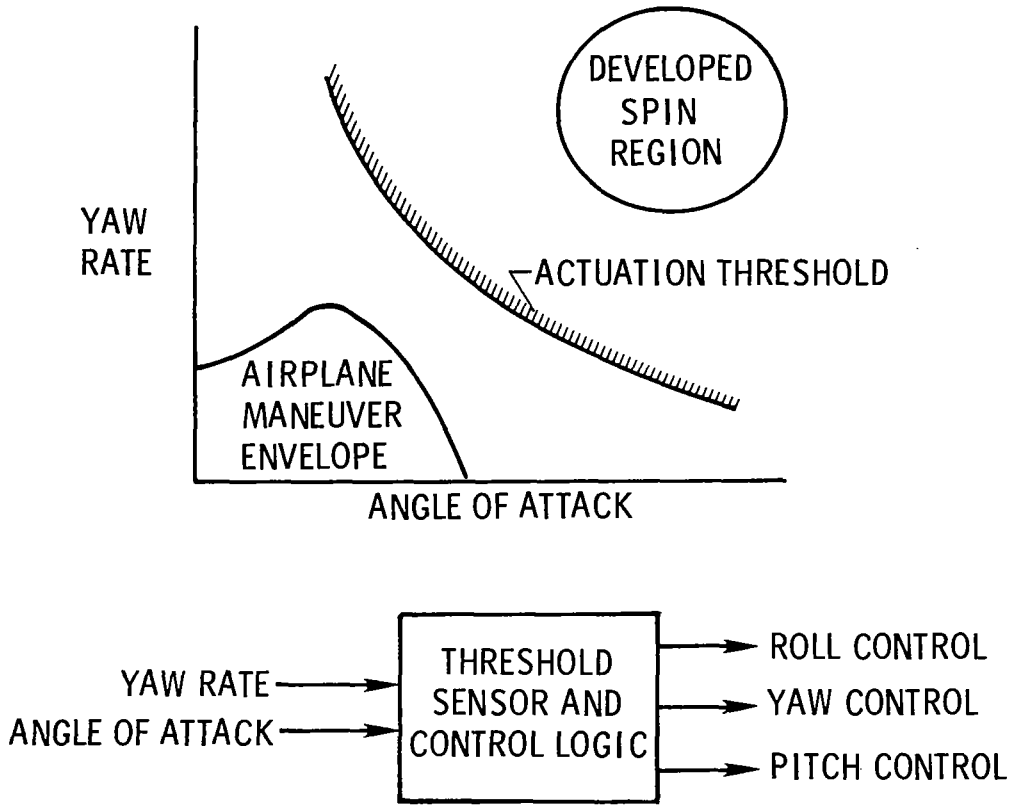

Figure 24.- Conceptual illustration of implementation of automatic spin-prevention systems.

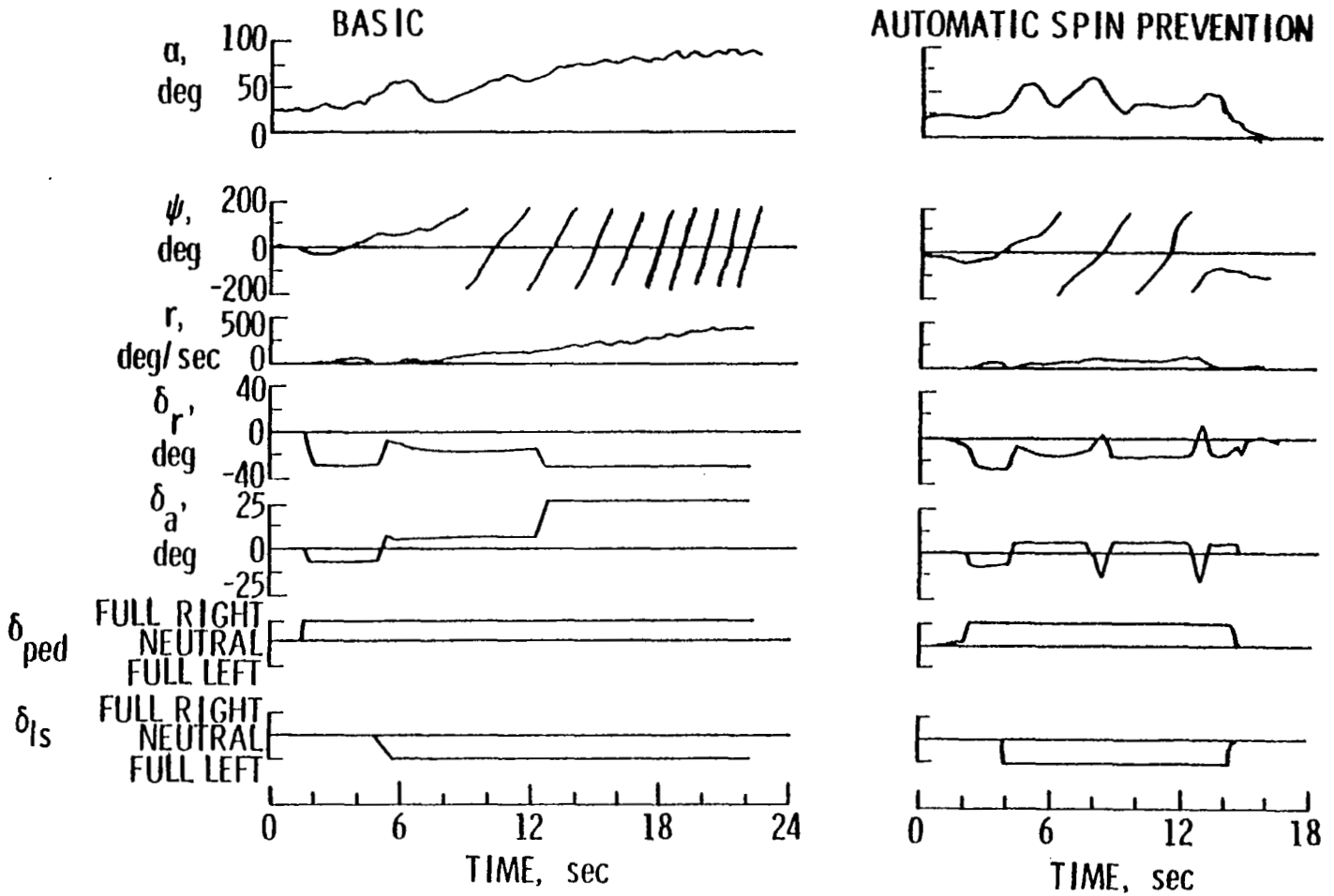

Figure 25.- Time histories of spin-entry attempts made on a free-flying dynamic model with and without an automatic spin-prevention system.

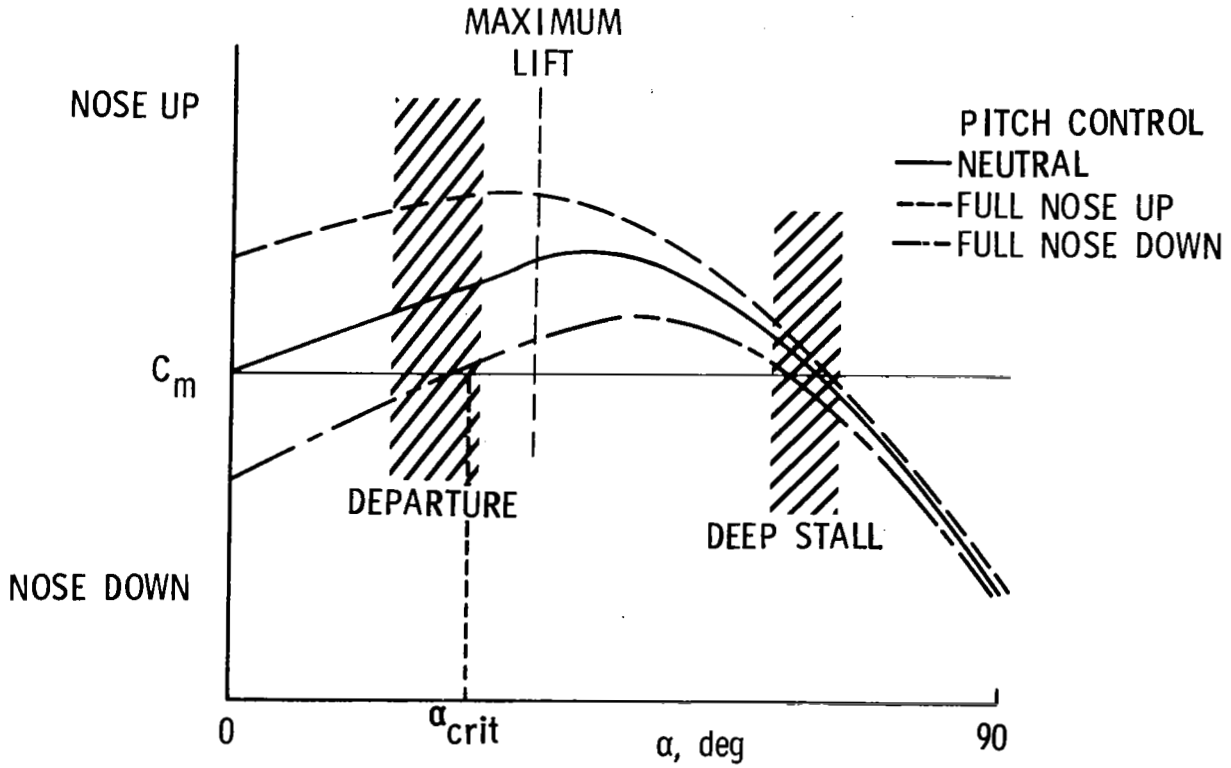

Figure 26.- Pitching-moment variation with α for idealized RSS configuration.

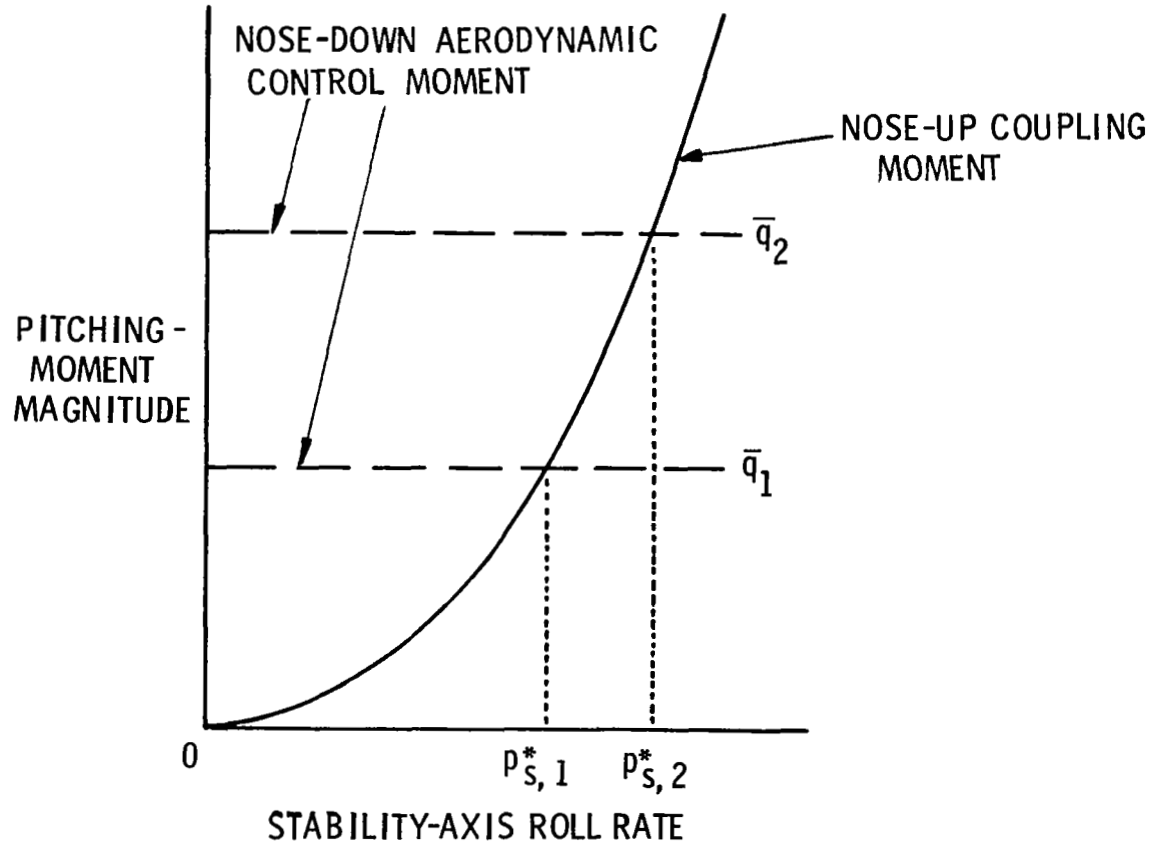

Figure 27.- Comparison of inertia-coupling moment for increasing roll rate with available aerodynamic pitch-control moment at two values of dynamic pressure.

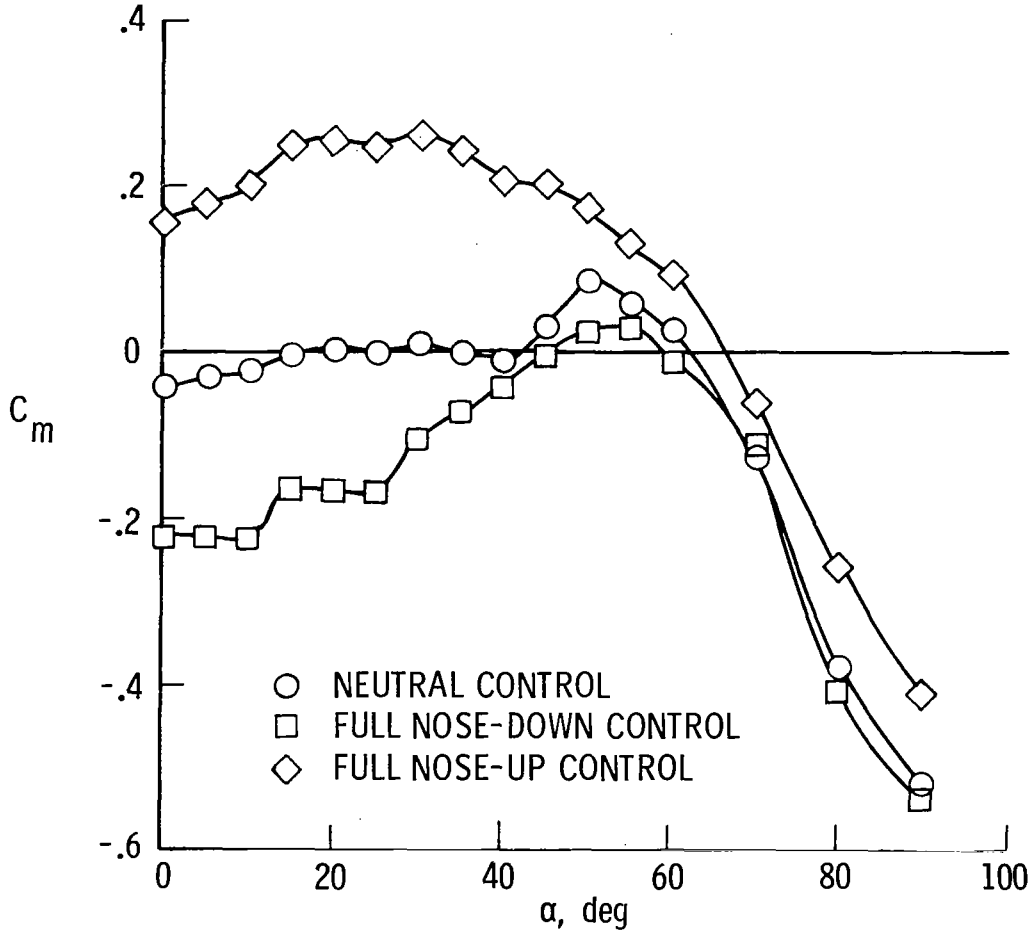

Figure 28.- Variation of pitching-moment coefficient with angle of attack for a fighter configuration incorporating RSS.

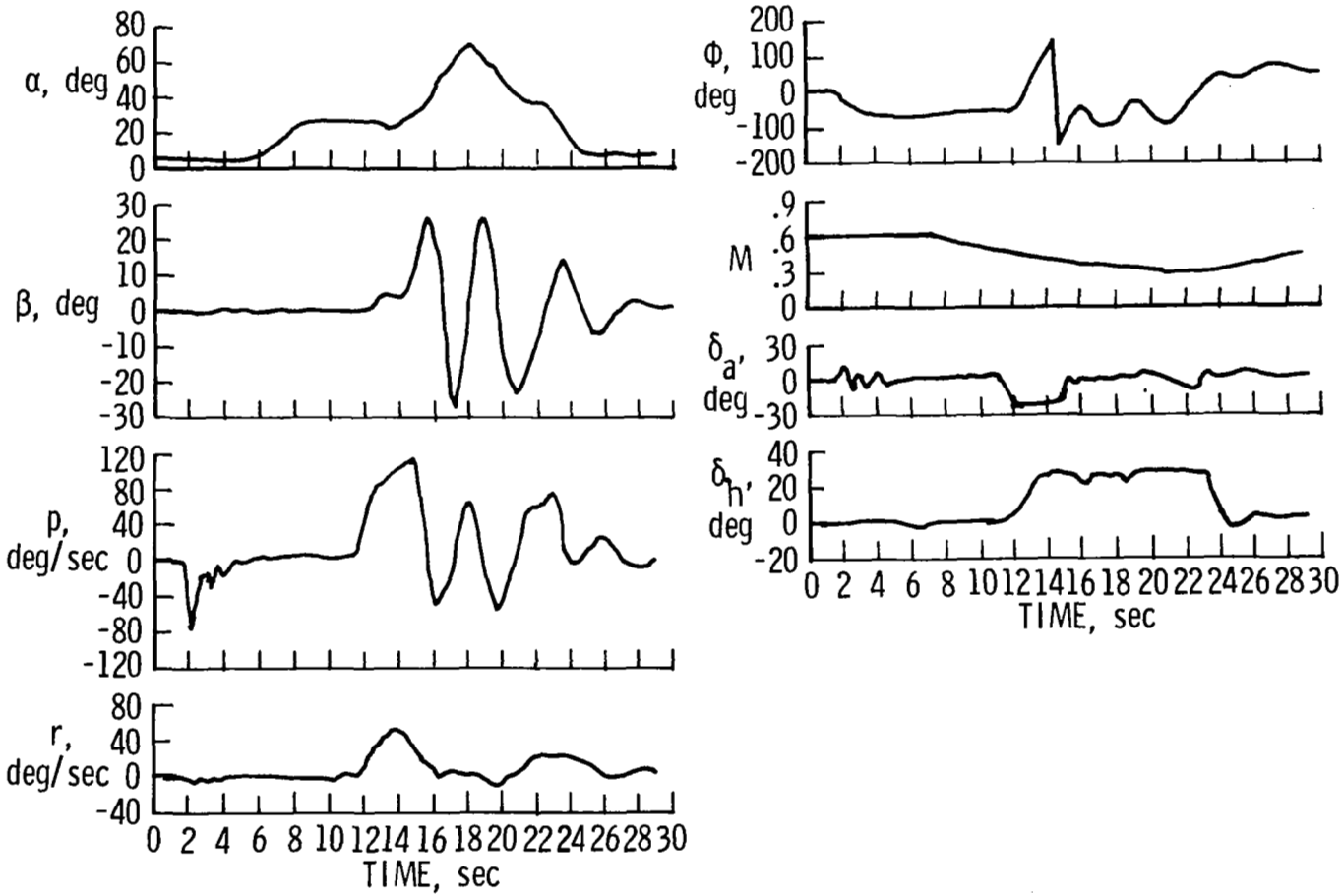

Figure 29.- Example of inertia-coupling pitch departure encountered during 360° roll attempt on fighter incorporating RSS.

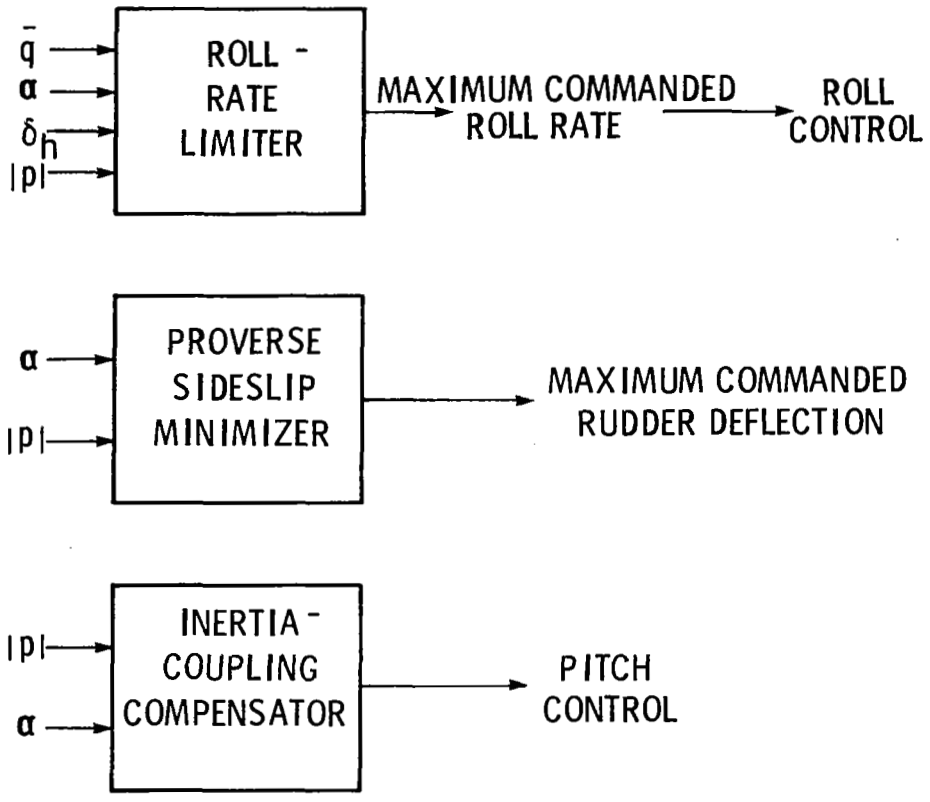

Figure 30.- Conceptual schematic of control-system features designed to inhibit high-angle-of-attack pitch departures.

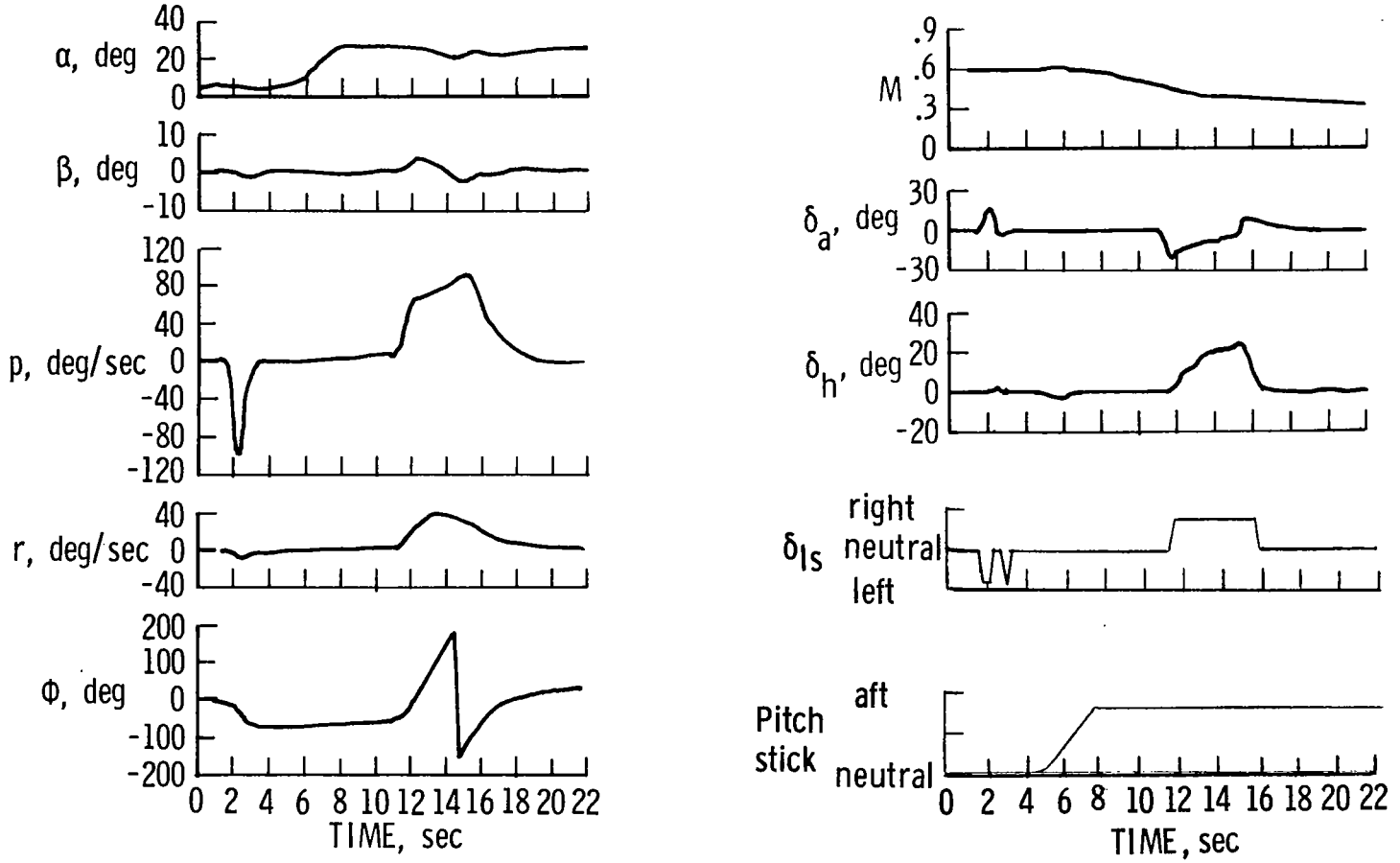

Figure 31.- Roll of 360° using full lateral-stick input on airplane equipped with pitch departure inhibitor system.

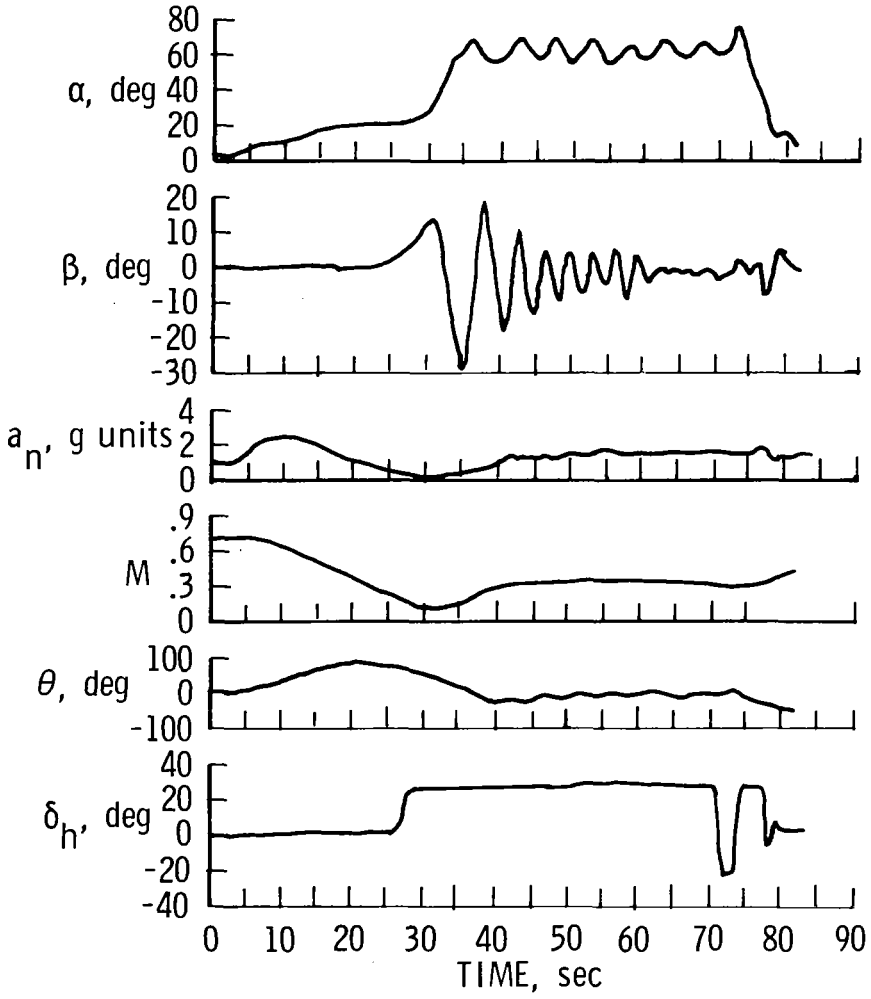

Figure 32.- Time histories of deep-stall recovery using pitch oscillation technique.

1. Report No. NASA TP-1689	2. Government Accession No.	3. Recipient's Catalog No.
4. Title and Subtitle CONTROL-SYSTEM TECHNIQUES FOR IMPROVED DEPARTURE/SPIN RESISTANCE FOR FIGHTER AIRCRAFT		5. Report Date August 1980 6. Performing Organization Code
7. Author(s) Luat T. Nguyen, William P. Gilbert, and Marilyn E. Ogburn		8. Performing Organization Report No. L-13453
9. Performing Organization Name and Address NASA Langley Research Center Hampton, VA 23665		10. Work Unit No. 505-43-13-01 11. Contract or Grant No.
12. Sponsoring Agency Name and Address National Aeronautics and Space Administration Washington, DC 20546		13. Type of Report and Period Covered Technical Paper 14. Sponsoring Agency Code
15. Supplementary Notes		

16. Abstract

This paper summarizes some fundamental information on control-system effects on controllability of highly maneuverable aircraft at high angles of attack and techniques for enhancing fighter aircraft departure/spin resistance using control-system design. The discussion includes (1) a brief review of pertinent high-angle-of-attack phenomena including aerodynamics, inertia coupling, and kinematic coupling, (2) effects of conventional stability augmentation systems at high angles of attack, (3) high-angle-of-attack control-system concepts designed to enhance departure/spin resistance, and (4) the outlook for applications of these concepts to future fighters, particularly those designs which incorporate relaxed static stability.

17. Key Words (Suggested by Author(s))	18. Distribution Statement
High angle of attack Control-system design Departure prevention Aircraft stability and control	Unclassified – Unlimited Subject Category 01

19. Security Classif. (of this report)	20. Security Classif. (of this page)	21. No. of Pages	22. Price*
Unclassified	Unclassified	66	A05

* For sale by the National Technical Information Service, Springfield, Virginia 22161

NASA-Langley, 1980

National Aeronautics and Space Administration

Washington, D.C.
20546

Official Business
Penalty for Private Use, $300

THIRD-CLASS BULK RATE

Postage and Fees Paid
National Aeronautics and
Space Administration
NASA-451

U.S.MAIL

3 1 1U,A, 072580 S00903DS
DEPT OF THE AIR FORCE
AF WEAPONS LABORATORY
ATTN: TECHNICAL LIBRARY (SUL)
KIRTLAND AFB NM 87117

NASA

POSTMASTER: If Undeliverable (Section 158 Postal Manual) Do Not Return